The Stability Region of the Tubing Performance Relation Curve.

Z.J.G. Gromotka

Faculty EEMSC

TU Delft Delft University of Technology

Challenge the future

THE STABILITY REGION OF THE TUBING PERFORMANCE RELATION CURVE.

by

Z.J.G. Gromotka

in partial fulfillment of the requirements for the degree of

Master of Science
in Applied Mathematics

at the Delft University of Technology,
to be defended publicly on Monday September 14, 2015 at 13:30.

Supervisors:	Dr. J. L. A. Dubbeldam and Dr. P. J. P. Egberts	
Thesis committee:	Prof. dr. ir. A. W. Heemink,	TU Delft
	Dr. J. L. A. Dubbeldam,	TU Delft
	Dr. D. R. van der Heul,	TU Delft
	Dr. P. J. P. Egberts,	TNO

This thesis is confidential and cannot be made public until -

TU Delft Delft University of Technology

TNO innovation for life

PREFACE

This report was done with the intention of receiving the title of Master of Applied Mathematics. After a year of research done at both the Technical University of Delft and TNO, this report is the culmination of my findings. Below is an abstract of my work:

The tubing performance relation curve is a measure of well performance in gas well engineering. It describes the two-phase flow inside a well and as such is modeled as a two-phase one dimensional pipe flow. Convention claims that production points on the TPR curve to the right of its minimum are stable. There also exist claims about the region slightly to the left of the minimum of the TPR curve being stable. To find the stability criteria the time behaviour of a small perturbation from the steady state conditions is modeled and studied. In the end the first claim was indeed verified but further research is suggested to determine if the stable region might be slightly larger.

I have learned a lot in that time and would like to thank my advisors, Johan and Paul, my family and my friends. I could not have made it this far without them. I hope this report enlightens you a bit more on the inner workings of gas well engineering as well as on two-phase flow inside pipes.

Z.J.G. Gromotka
Delft, September 2015

CONTENTS

INTRODUCTION

In this thesis report the inner workings of flow inside a gas well are described and studied. A gas well that produces only gas is called a dry gas well, however dry gas wells are not common. The gas flow will often contain traces of liquid, i.e. water, gas condensate or both. Too much liquid can hinder the flow and thus the production of gas.
One way of seeing the effect liquid has on the flow is to look at the flow regime. As the liquid ratio increases the flow regime changes. In figure 1 the flow regimes for vertical flow are displayed. They are discussed by increasing liquid ratio, form right to left, beginning with annular flow. For low liquid ratios and high gas flow

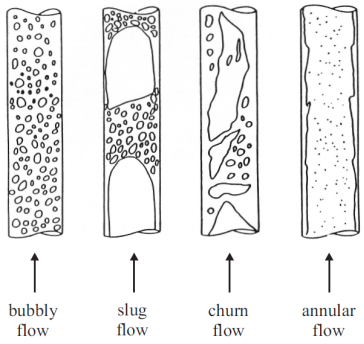

Figure 1: Flow regimes for vertical pipe flow from [1]

rates the majority of liquid will collect on the inner pipe, with small bubbles of liquid distributed over the gas flow in the center. Churn flow is a highly volatile flow in the transition region from annular flow to slug flow. Slug flow is the flow of big bullet shaped bubbles intermitted by pockets of liquid carrying smaller bubbles of gas. Bubble flow results from high liquid ratios where the gas is hindered by the fluid and travels at low flow rate. As the amount of liquid increases it will be more difficult for gas to travel through it, until there is a column of liquid blocking all gas production. This phenomenon is called liquid loading, see figure 2.

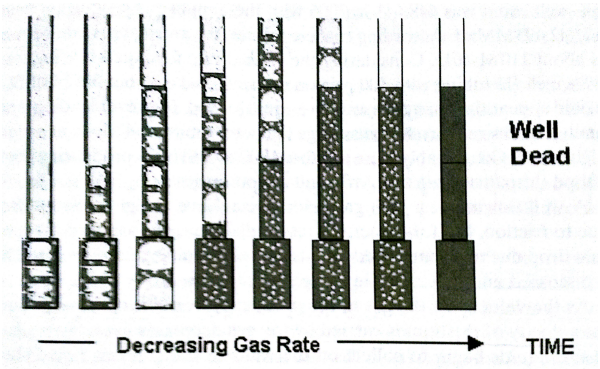

Figure 2: Depiction of liquid loading from [2]

While gas production is possible at low flow rates it might not be economically beneficial to maintain a well that produces at such low rates. Also flow with a low flow rate is considered unstable, as a small change in the conditions of the well, fluid, or reservoir, can increase the liquid ratio leading to eventual well death. Flows with a higher flow rate tend to react better to a change in one of the many variables influencing the flow, as they eventually adjust back to a original production rate.
The production rate is determined by the well as well as the reservoir. Possible steady state production conditions for the well are given by the tubing performance relation (TPR) curve. The shape of the TPR curve in

turn is dependent on the relation between flow rate and liquid ratio. This report tries to answer the question, how the stability of the production rate and the shape of the TPR curve are connected.

In the first chapter some background information is given. The coupling of the gas and reservoir are discussed and what makes a production point stable. In the second chapter the problem is translated to mathematics. In the third chapter the tubing performance relation curve is discussed and derived from the conservation equations in fluid dynamics. The fourth chapter discusses nodal analysis and if the stability argument given holds. The fifth chapter tries to study the behaviour of perturbations to the steady state system. Finally, a conclusion is given and further extensions to the model are discussed.

1

BACKGROUND KNOWLEDGE

In this chapter several terms, ideas and analysis techniques, from gas reservoir engineering, are introduced. These provide insight into the problem, help define the idea of stability and explain current conventions.

1.1. TUBING PERFORMANCE RELATION CURVE

A well's production is dependent on the mechanical configuration of the wellbore, the fluid properties, the reservoir conditions and several other factors. There are several ways to determine the well's performance. One way is the tubing performance relation (TPR) curve, also known as the tubing performance curve (TPC), the vertical lift performance and the outflow performance curve.

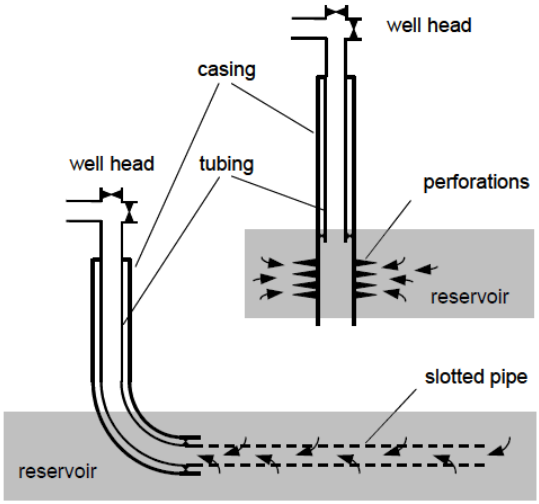

Figure 1.1: Two simplified dipictions of gas well-reservoirs system from [3]

There are two versions of the TPR curve used in practice. The first depicts the relation between the pressure drop of the well and the flow rate at the well head shown in figure 1.1, i.e. the top site flow rate. This is the version used in this report. The second depicts the relation between the bottom hole pressure and the top site flow rate. This second curve just adds the well head pressure to the pressure drop to give the actual pressure at the bottom of the well. It is merely the first curve plus a constant.
In general the pressure drop is determined using the mechanical energy equation [4, 5] for flow between two points of the system,

$$\frac{p_1}{\rho} + gz_1 + \frac{u_1^2}{2} = \frac{p_2}{\rho} + gz_2 + \frac{u_2^2}{2} + W + E_l. \tag{1.1}$$

With the variables p, u, z, ρ, g, W and E_l representing respectively pressure, flow rate, depth, density, gravitational acceleration, work on the fluid and the irreversible energy loses. Where the subscripts 1 and 2 denote

the location within the system. For the setup in this report the mass conservation and momentum conservation are used instead of the mechanical energy equation. This may be done since the mechanical energy equation is equivalent to the steady state momentum conservation equation C,
As mentioned in the introduction, the fluid inside the gas well often contains liquid, i.e. there is two-phase flow. This results in a specific shape for the TPR curve. The pressure drop over the well needs to be large enough to compensate the forces working on the fluid. At low flow rates the gravitational force is large due to the large ratio of liquid. At high flow rates the frictional force between the fluid and the well is large. This results in what is often called a J-curve as in figure 1.2 below.

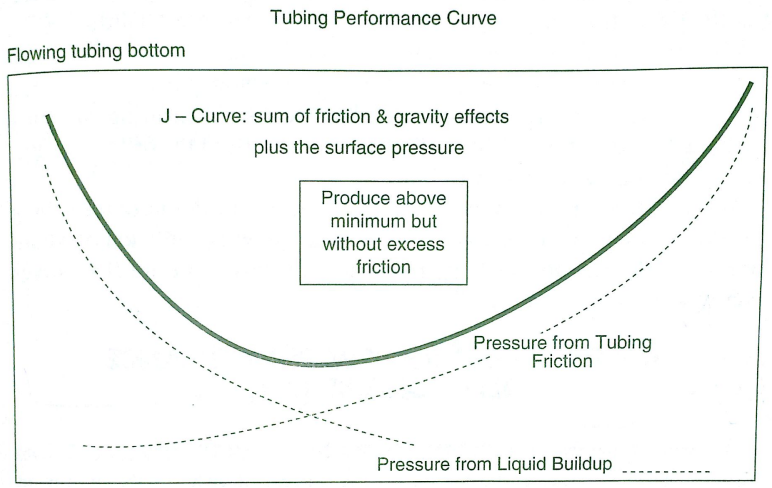

Figure 1.2: Standard shape of the TPR curve from [2]

The TPR curve is a combination of all possible steady state production conditions for the well, given certain conditions. To determine the actual or natural production conditions the characteristics of the reservoir need to be taken into account. The next section explains the inflow performance relation curve which represents the possible production conditions of the reservoir. And it will link both curves to determine natural production.

1.2. INFLOW PERFORMANCE RELATION CURVE

The inflow performance relation (IPR) curve is another way to determine the well's production performance, or rather the reservoirs production performance. The IPR curve plots the flow rate against the bottom hole pressure. When the bottom hole pressure is equal to the reservoir pressure the flow rate is zero and the maximum flow rate is given there where the bottom hole pressure is zero. For oil reservoirs the IPR curve is often a straight line connecting these two points. For gas reservoirs however, the curve is more arched, see figure 1.3. The backpressure equation given in [2], explains this curved shape,

$$q = C\left(p_r^2 - p_{wf}^2\right)^n. \tag{1.2}$$

Here q is the flow rate, p_r is the reservoir pressure and p_{wf} is the bottom hole pressure. While C and n are empirical parameters obtained from measurements at the reservoir.
Now if the TPR and the IPR curve both plot the bottom hole pressure they can be shown in one graph as in figure 1.4. The points where the two curves coincide show the natural production rates. The amount of natural production points can be zero, one and even two. If there are two natural production points, however, one is often unstable.
A natural production point is called stable, if the flow adjusts back to the natural production point after a slight perturbation from natural production conditions. Otherwise it is considered unstable. The rule of thumb is that the flow rate to the left of the minimum of the TPR curve is unstable. The stability is generally studied using nodal analysis. However, even in that field some adjustments have been made to the claim, saying stable production is possible slightly left of the minimum of the TPR curve.
This report will further explore the possibility of a bigger region of stability for the TPR curve. But first, the

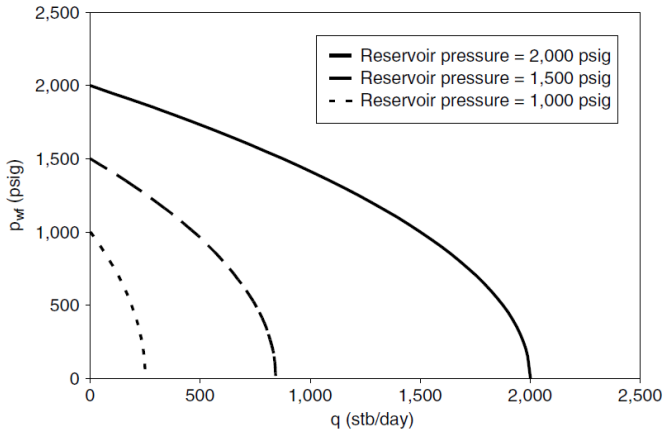

Figure 1.3: Examples of IPR curves for gas reservoirs from [5]

next chapter will derive the mathematical system describing the flow. After which TPR curve and its stability is studied further.

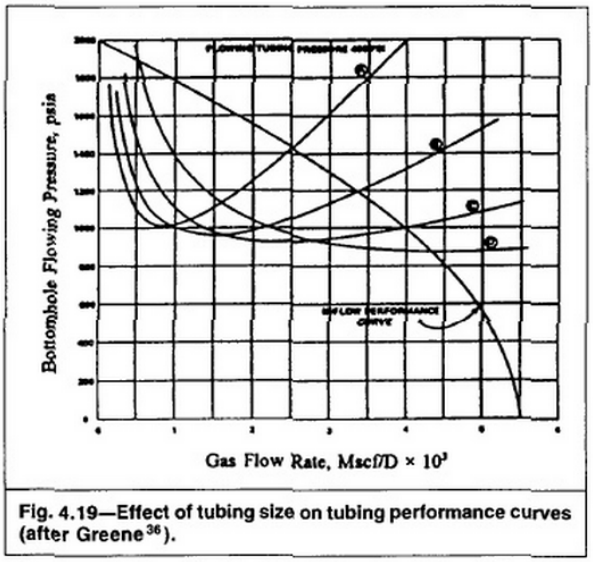

Figure 1.4: Examples of TPR curves for different tubing sizes, along with the IPR from [4]

2

THE MATHEMATICAL MODEL SETUP

In this chapter a mathematical model is set up using the main principles of fluid dynamics. Fluid dynamics is the study of a fluid in motion. Different types of flow and fluids will be discussed and a general model for two-phase flow in a pipe will be derived.

2.1. CONSERVATION EQUATIONS

To describe fluid flow, fluid dynamics states the conservation laws. The three conservation laws considered are, mass conservation, momentum conservation and energy conservation. These conservation laws are expressed using the Euler equations below. Euler equations are simplified version of Navier-stokes equations and are generally used for modeling gas well problems [1]. For the Euler equations some assumptions apply: there is no mass source present inside the domain, and the flow is inviscid B.1.

$$\partial_t \rho + \nabla \cdot (\rho \mathbf{u}) = 0, \tag{2.1}$$

$$\partial_t (\rho \mathbf{u}) + \nabla \cdot (\rho \mathbf{u})\mathbf{u} + \nabla p = \mathbf{F}, \tag{2.2}$$

$$\partial_t (E) + \nabla \cdot (E + p)\mathbf{u} = \mathbf{F}\mathbf{u}. \tag{2.3}$$

The three equations have four unknown variables, ρ, $\mathbf{u}$, p and E, and a forcing term, F. Representing respectively,

- ρ: density, $\mathrm{kg\,m^{-3}}$,
- $\mathbf{u}$: vector of flow rate, $\mathrm{m\,s^{-1}}$,
- p: pressure, $\mathrm{kg\,m^{-1}\,s^{-2}}$,
- E: total energy, J,
- $\mathbf{F}$: vector of net body forces, N.

In the next section the body net forces $\mathbf{F}$ present in equations (2.2) and (2.3) are given and further elaborated on. The flow is assumed isothermal in which case equation (2.3) may not be neglected. The energy conservation equation may however be replaced by the equation of state for gases presented in section 2.3. For this reason equation (2.3) is dropped to be replaced later. For now the system is reduced to two partial differential equations (2.1) and (2.2), instead of three, with unknown variables, ρ, $\mathbf{u}$ and p. This system holds in general but as mentioned before, this is a two phase flow problem. How this effects these equations is covered later in the chapter.

2.2. BODY NET FORCES F

To know which forces are working on the fluid, the domain and geometry of the problem need to be specified. Since the goal is to construct the Tubing Performance Relation (TPR) curve, the domain is the well tubing i.e. the inside of the well. This region is similar to a cylindrical pipe. To keep the geometry simple the well is considered straight, with constant diameter D. Its length L is taken from above the well perforations up to

the surface, and is known to be much larger than the diameter, i.e. $L \gg D$. A schematic representation of the geometry of the domain is given in figure 2.1. To determine the domain the z-axis is taken along the length of the well, with $z = 0$ at the reservoir side of the pipe and $z = L$ at the surface side. Then domain for this problem is $\Omega = \{(x, y, z) \in \mathbb{R} : \ x^2 + y^2 = D^2/4, \ 0 \le z \le L\}$. Since there is no flow out the casing of the pipe the

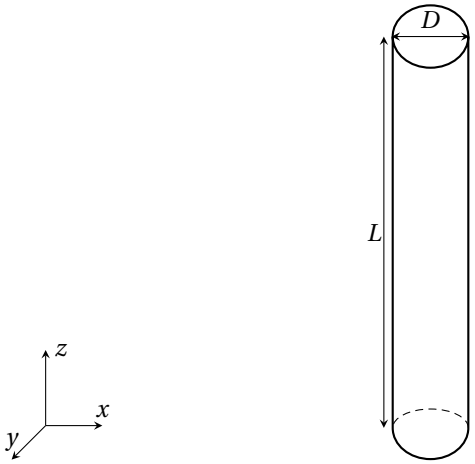

Figure 2.1: Simplified geometry of the inside of the well

flow in the x, y-direction is not very interesting. Therefore the variables are taken as averages over the wells' cross sectional area A. This results in the flow rate $\mathbf{u}$ and the net body force $\mathbf{F}$ having only one non-zero element, specifically in the z-direction. Thus the problem is reduced to one spatial dimension and the domain of interest is condensed to $\Omega = \{z \in \mathbb{R} : 0 \le z \le L\}$.

For flow inside a pipe the body net forces will consist of a gravitational force F_g and a frictional force F_w, caused by the contact with the inside wall of the pipe. Note that $A\rho$ is the mass per meter of pipe and thus $A\rho u = Q$ is the mass flow rate in $\mathrm{kg\,s^{-1}}$. Therefore the mass and momentum conservation equations for one dimensional pipe flow are given by,

$$\partial_t(A\rho) + \partial_z(A\rho u) = 0, \tag{2.4}$$

$$\partial_t(A\rho u) + \partial_z(A\rho u^2) + A\partial_z p = -\Big(\underbrace{A\rho g}_{F_g} + \underbrace{\tau_w S}_{F_w}\Big). \tag{2.5}$$

With the new variables and parameters introduced listed and defined below,

- u: flow rate averaged over the cross-section, $\mathrm{m\,s^{-1}}$,
- A: pipe cross-sectional area, $\mathrm{m^2}$,
- S: pipe perimeter, m,
- g: gravitational acceleration, $\mathrm{m\,s^{-2}}$,
- τ_w: shear stress at the pipe wall, $\mathrm{kg\,m^{-1}\,s^{-2}}$.

The gravitational force and the gravitational acceleration are commonly known. However a well does not have to run vertically, in that case the gravitational acceleration is adjusted for the angle θ, $g \to g\sin(\theta)$. The shear stress τ_w will be further elaborated on in the next subsection.

The conservation equations (2.4) and (2.5) are rewritten, taking into account the assumption that the cross-sectional area A is constant over the domain, i.e. the length L of the pipe.

$$\partial_t\rho + \partial_z(\rho u) = 0, \tag{2.6}$$

$$u\big(\partial_t\rho + \partial_z(\rho u)\big) + \rho\left(\partial_t u + u\partial_z u\right) + \partial_z p = -\left(\rho g + \tau_w \frac{S}{A}\right). \tag{2.7}$$

The first term of equation (2.7) is equal to zero. So the system can be reduced to,

$$\partial_t \rho + \partial_z(\rho u) = 0, \tag{2.8}$$

$$\rho\left(\partial_t u + u\partial_z u\right) + \partial_z p = -\left(\rho g + \tau_w \frac{S}{A}\right). \tag{2.9}$$

2.2.1. FRICTIONAL FORCE

The frictional force on the flow is a consequence of the shear stress between the wall of the pipe and the fluid. By definition a Newtonian fluid (see Definition B.3) has a wall shear stress τ_w proportional to the acceleration of the flow towards the middle of the pipe. If the velocity profile is assumed parabolic then for a fully laminar flow (see Definition B.2) in a cylindrical pipe, the wall shear stress is known as

$$\tau_w = 8\mu\frac{u}{D}. \tag{2.10}$$

With μ the fluid viscosity. For other flow regimes the relation between the average (over the cross section) flow rate and the actual flow rate is not explicitly known. Therefore a more general expression of the shear stress is introduced,

$$\tau_w = \frac{f\rho u^2}{2}. \tag{2.11}$$

Here f is the Fanning friction factor, a dimensionless variable that is dependent on the Reynolds number, $Re = \frac{\rho u D}{\mu}$ and the pipes relative roughness, $\frac{\varepsilon}{D}$, with ε the absolute roughness. For a laminar flow regime the fanning friction is easily calculated since the shear stress is known (2.10),

$$f = 16\frac{\mu}{\rho u D} = \frac{16}{Re}. \tag{2.12}$$

In general there are two ways to determine the Fanning friction factor for turbulent flow regimes. The first is using an empirical expression. A commonly used expression is the Colebrook [6] equation, which is accurate for turbulent flow regimes with $Re \geq 2300$,

$$\frac{1}{\sqrt{f}} = -4\log\left(\frac{2\varepsilon}{D} + \frac{9.35}{Re\sqrt{f}}\right) + 3.48. \tag{2.13}$$

The Colebrook equation (2.13) is implicit and is solved iteratively. For industrial applications a decent accuracy can be achieved within 10 iterations. Literature presents several explicit alternatives to the Colebrook equation. However many of these alternatives are merely explicit approximations of the Colebrook equation. One approximation worth mentioning though, is that of Churchill [7],

$$\begin{aligned} f =& 2\left[\left(\frac{8}{Re}\right)^{12} + \frac{1}{(a+b)^{3/2}}\right]^{1/12}, \qquad \text{with} \\ a =& \left[2.457\ln\left(\left(\frac{7}{Re}\right)^{0.9} + 0.27\frac{\varepsilon}{D}\right)\right]^{16}, \quad \text{and} \\ b =& \left(\frac{37530}{Re}\right)^{16}. \end{aligned} \tag{2.14}$$

The Churchill equation (2.14) holds for both laminar flow as well as turbulent flow. It combines the expression for laminar flow (2.12) and the Colebrook expression (2.13), including estimates for the transitional flow regime starting at $Re = 2100$.

The second way to determine the Fanning friction factor is to use the Moody diagram shown in figure 2.2. The Moody diagram plots the Moody friction factor for given Reynolds number en relative roughness. The Moody friction factor, also known as the Darcy friction factor or the Darcy-Weisbach friction factor, is four times the Fanning friction factor, $4f_{Fanning} = f_{Moody}$.

Using expression (2.11) for the the shear stress τ_w, the momentum conservation equation (2.9) becomes

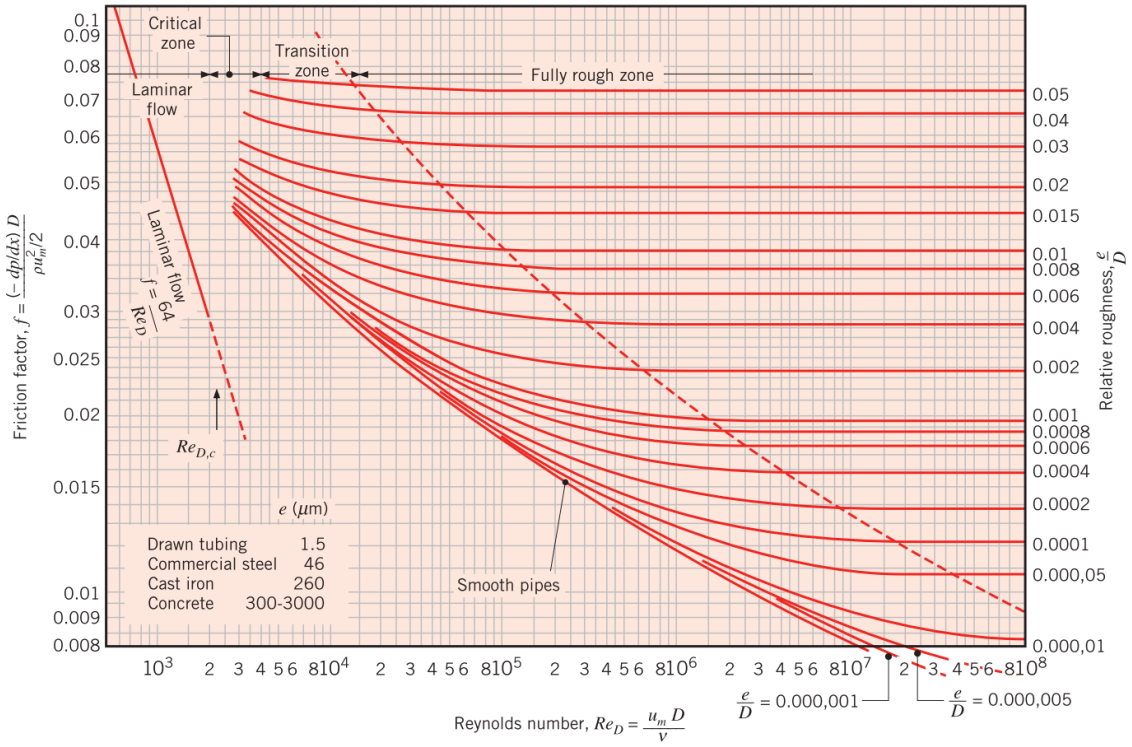

Figure 2.2: The Moody diagram taken from [8]

$$\begin{cases} \rho\left(\partial_t u + u\partial_z u\right) + \partial_z p = -\rho\left(g + \frac{2fu^2}{D}\right), & \text{for all flow regimes,} \\ \rho\left(\partial_t u + u\partial_z u\right) + \partial_z p = -\rho\left(g + \frac{32u^2}{ReD}\right), & \text{for a laminar flow regime.} \end{cases} \tag{2.15}$$

The next section will show how the mass conservation (2.6) and the momentum conservation (2.15) change when the fluid is two-phase.

2.3. TWO-PHASE FLOW

As discussed in the introduction the flow inside the well is a two phase flow. While equations (2.6) and (2.15) hold in general, it is still a two equation system with three unknown variables. A closure relation is needed to complete this system. The flow is isothermal and the closure relation comes from the equation of state for gasses, i.e. equation (2.16). So first the gas phase and liquid phase properties are discussed separately after which a coupling is made to the two phase fluid properties.

$$\rho_g = \frac{p}{zRT}. \tag{2.16}$$

With R the specific gas constant $\mathrm{J\,kg^{-1}\,K^{-1}}$, T the temperature K and z the compressibility factor. The compressibility factor is the ratio of molar volume actual gas to the molar volume of ideal gas and is a function of the pressure p as well as a function of the temperature T. For ideal gasses where $z = 1$ equation (2.16) reduces to the ideal gas law.

In chapter one of [4] the relation between the compressibility factor z and the pressure p is plotted similaly to figure 2.3 for several temperatures T. The higher the temperature the flatter the z, p-curve, i.e. an almost constant compressibility factor z. Due to the isothermal flow assumption the temperature T is constant. For these type of gas well engineering problems [4] the gas compressibility factor z is averaged over the domain. Using the averaged compressibility factor z_{avg} instead of z a new constant parameter c_g and

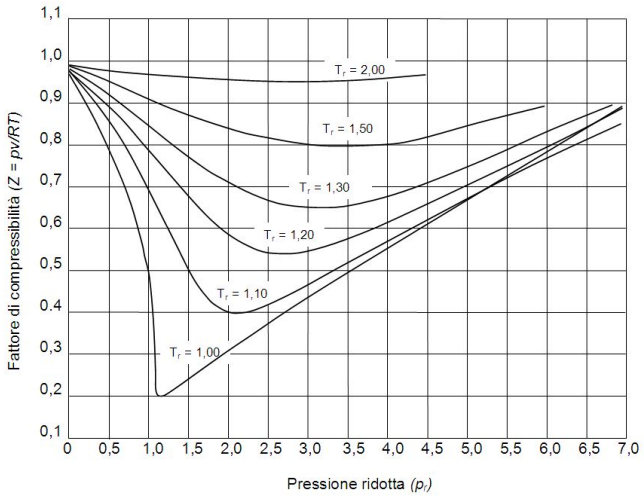

Figure 2.3: A generalized diagram of the compressibility factor z from [9]

equation of state can be introduced,

$$c_g = \sqrt{z_{avg} RT}, \tag{2.17}$$

$$p = c_g^2 \rho_g. \tag{2.18}$$

If the gas is an ideal gas the parameter c_g is equivalent to the speed of sound in the gas. If not the parameter c_g is merely an umbrella variable to reduce the number of parameters.

Assuming there is no mass transfer between the two phases, the liquid will be strictly incompressible, i.e. ρ_l is constant in space and time. Now to define the mixture density as the average of both phase densities,

$$\rho_m = \alpha_g \rho_g + \alpha_l \rho_l. \tag{2.19}$$

Where α_i is the fraction of phase $i = l, g$, across the cross-section A of the pipe. To define these fractions mathematically we introduce a new variable,

$$\alpha = \frac{1}{A} \iint_A \mathbb{1}_g \, \mathrm{d}\Gamma. \tag{2.20}$$

Where α is the fraction of gas across the cross-section A, and may be height z dependent. Now the fraction of the gas phase and that of the liquid phase are defined as $\alpha_g = \alpha$ and $\alpha_l = 1 - \alpha$ respectively.

The average mixture flow rate can be defined by starting from the x, y dependency. The flow rate before averaging over the cross-section is denoted by $u^{x,y}$, so

$$u_m = \frac{1}{A} \iint_A u^{x,y} \, \mathrm{d}\Gamma, \tag{2.21}$$

$$= \frac{1}{A} \iint_A u^{x,y} \mathbb{1}_g + u^{x,y} \mathbb{1}_l \, \mathrm{d}\Gamma, \tag{2.22}$$

$$= \frac{1}{A} \iint_A u_g^{x,y} + u_l^{x,y} \, \mathrm{d}\Gamma, \tag{2.23}$$

$$= \alpha_g u_g + \alpha_l u_l. \tag{2.24}$$

Note that the averaged phase flow rate u_i is not averaged over the entire cross-section A. Instead it is averaged over the area $\alpha_i A$ where the phase is present,

$$u_i = \frac{1}{\alpha_i A} \iint_A u_i^{x,y} \, \mathrm{d}\Gamma, \qquad i = l, g, \tag{2.25}$$

$$= \frac{1}{A} \iint_A u_{i/\alpha}^{x,y} \, \mathrm{d}\Gamma. \tag{2.26}$$

Where $u_{i/\alpha}^{x,y} = \frac{u_i^{x,y}}{\alpha_i}$. The phase flow rate averaged over the whole cross-section is called the superficial phase flow rate, and is explained as the flow rate under the assumption no other phases are present,

$$u_{si} = \frac{1}{A}\iint_A u_i^{x,y}\,\mathrm{d}\Gamma, \qquad i = l, g. \tag{2.27}$$

To link the gas flow rate u_g to the mixture flow rate u_m, the drift flow rate $u_d^{x,y}$ is first introduced,

$$u_d^{x,y} = u_{g/\alpha}^{x,y} - u^{x,y}. \tag{2.28}$$

Doing some simple manipulation one can find a expression for the gas flow rate u_g,

$$u_g = \frac{\iint_A u_g^{x,y}\,\mathrm{d}\Gamma}{\alpha A} \tag{2.29}$$

$$= \frac{\iint_A \alpha u^{x,y}\,\mathrm{d}\Gamma}{\alpha A u_m} u_m + \frac{\iint_A \alpha u_d^{x,y}\,\mathrm{d}\Gamma}{\alpha A}, \tag{2.30}$$

$$= C_0 u_m + u_b. \tag{2.31}$$

Where

$$C_0 = \frac{\iint_A \alpha u^{x,y}\,\mathrm{d}\Gamma}{\alpha A u_m} \quad \text{and} \quad u_b = \frac{\iint_A \alpha u_d^{x,y}\,\mathrm{d}\Gamma}{\alpha A}. \tag{2.32}$$

The parameter C_0 is the distribution correlation and is linked to the flow regime. Values for C_0 vary between 1 and 1.25. Empirically expressions for C_0 are often found to be dependent on the density ratio $\frac{\rho_g}{\rho_l}$, where C_0 is one for equal phase densities, see [1, 10–12] for examples. The parameter u_b is the weighted mean drift flow rate and is usually dependent on the density difference $\Delta\rho = \rho_l - \rho_g$. This parameter is also found empirically [1, 10–12].

Using this information the drift-flux model is set up. The drift-flux model uses both single phase mass conservation equations and a mixed momentum conservation equation. For the mixed conservation momentum equation the mixture fanning friction factor f_m is determined using a mixture Reynolds number, $Re_m = \frac{\rho_m u_m}{\mu_l}$ assuming $\mu_l \gg \mu_g$. The drift-flux model states,

$$\partial_t[(1-\alpha)\rho_l] + \partial_z[(1-\alpha)\rho_l u_l] = 0, \tag{2.33}$$

$$\partial_t(\alpha\rho_g) + \partial_z(\alpha\rho_g u_g) = 0, \tag{2.34}$$

$$\rho_m(\partial_t u_m + u_m\partial_z u_m) + \partial_z p = -\rho_m\left(g + \frac{2f_m u_m^2}{D}\right). \tag{2.35}$$

This set of equations can be expressed in terms of three unknown variables, one example is (p, u_m, α), which gives

$$-\partial_t\alpha + \partial_z\left[(1-\alpha C_0)\,u_m\right] = 0, \tag{2.36}$$

$$\partial_t\alpha p + \partial_z[\alpha p C_0 u_m] = 0, \tag{2.37}$$

$$\rho_m(\partial_t u_m + u_m\partial_z u_m) + \partial_z p = -\rho_m\left(g + \frac{2f_m u_m^2}{D}\right). \tag{2.38}$$

Where C_0, f_m and D are assumed to be known constants and ρ_m is a function (2.19) of the unknown variables. Analysing and possibly solving a system of three equations though possible, is strenuous work. If one can connect the superficial flow rates of both phases (see Equation (2.27)) then there exists an explicit expression for α, thereby reducing the number of unknowns.

The variable α can be expressed using the superficial gas flow rate and gas flow rate,

$$\alpha = \frac{u_{sg}}{u_g} = \frac{u_{sg}}{C_0 u_m + u_b}. \tag{2.39}$$

Since the mixture flow rate is the sum of both superficial flow rates, $u_m = u_{sg} + u_{sl}$, finding an expression for the liquid superficial flow rate should be enough to reduce the number of unknowns. Instead of looking for an

expression using data or empirical relations the choice was made to study a simple linear relation. Knowing the liquid flow rate is less than the gas flow rate for all α, the assumption is made that this relation translates to the superficial flow rates. The following relations are chosen,

$$u_{sl} = q u_{sg}, \tag{2.40}$$

$$u_{sg} = \frac{u_m}{1+q}, \tag{2.41}$$

where $0 < q \leq 1$ is a scaling variable. Using equation (2.41) the variable α can be expressed in either u_{sg} or u_m. The choice is made to model the mixture flow rate further. Then

$$\alpha = \frac{u_m}{(C_0 u_m + u_b)(1+q)}, \tag{2.42}$$

$$\alpha = \frac{u_m}{\hat{C}_0 u_m + \hat{u}_b}. \tag{2.43}$$

Using this relation for α, the homogenous equilibrium model (HEM) is setup,

$$\partial_t \rho_m + \partial_z (\rho_m u) = 0 \tag{2.44}$$

$$\rho_m (\partial_t u_m + u_m \partial_z u_m) + \partial_z p = -\rho_m \left(g + \frac{2 f_m u_m^2}{D} \right), \tag{2.45}$$

$$\rho_m = \alpha \frac{p}{c_g^2} + (1-\alpha)\rho_l. \tag{2.46}$$

Note for the rest of the report the subscript m will be dropped as the variables will always refer to the mixture properties unless stated otherwise. The HEM equations (2.44) and (2.45) are no different from the single phase representation of equations (2.6) and (2.15). The two phase fluid properties only become apparent in the closure relation (2.46). The next section will derive the dimensionless representation of these last three equations (2.44), (2.45) and (2.46).

2.4. DIMENSIONLESS EQUATIONS

The variables of equations (2.44) and (2.45) will be scaled using the characteristic length, speed and density respectively,

$$L = D \qquad \text{the pipe diameter} \tag{2.47}$$

$$U = u_{ref} \qquad \text{a reference velocity} \tag{2.48}$$

$$R = \rho_l \qquad \text{the liquid density} \tag{2.49}$$

In general the reference length would be equal to the hydraulic diameter. The hydraulic diameter in turn is a parameter that relates the perimeter of the pipe to the area of the pipe. For a cylindrical pipe the hydraulic pipe diameter is equal to the actual pipe diameter D. The choice for the reference velocity u_{ref} will be discussed later on.

Define the dimensionless variables as

$$z^* = \frac{z}{L} \qquad u^* = \frac{u}{U} \qquad \rho^* = \frac{\rho}{R} \qquad t^* = \frac{tU}{L} \qquad p^* = \frac{p}{RU^2}$$

Then the dimensionless mass conservation equation will be

$$\frac{RU}{L}\partial_{t^*}\rho^* + \frac{RU}{L}\partial_{z^*}(\rho^* u^*) = 0, \tag{2.50}$$

$$\partial_{t^*}\rho^* + \partial_{z^*}(\rho^* u^*) = 0. \tag{2.51}$$

And the dimensionless momentum conservation equation will be

$$\frac{RU^2}{L}\rho^*\partial_{t^*}u^* + \frac{RU^2}{L}\rho^* u^* \partial_{z^*}u^* + \frac{RU^2}{L}\partial_{z^*}p^* + RU^2\frac{2f}{D}\rho^*(u^*)^2 + R\rho^* g = 0, \tag{2.52}$$

$$\rho^*\partial_{t^*}u^* + \rho^* u^* \partial_{z^*}u^* + \partial_{z^*}p^* + 2f(u^*)^2 + \frac{\rho^*}{Fr} = 0. \tag{2.53}$$

Where $Fr = \frac{U^2}{Lg}$ is the Froude number. Lastly the dimensionless closure relation is

$$R\rho^* = \alpha \frac{RU^2}{c_g^2} p^* + (1-\alpha)\rho_l, \tag{2.54}$$

$$\rho^* = \alpha M^2 p^* + (1-\alpha). \tag{2.55}$$

Where $M = \frac{U}{c_g}$ is the Mach number. Aside from the model equations, it is also interesting to see how the scaling changes the expressions for the mixture flow rate,

$$Uu^* = u_{sg} + u_{sl} = \alpha u_g + (1-\alpha)u_l, \tag{2.56}$$

$$= u_{sg}^* + u_{sl}^* = \alpha u_g^* + (1-\alpha)u_l^*. \tag{2.57}$$

All phase flow rates and superficial phase flow rates are scaled with the reference velocity $U = u_{ref}$. This can again be seen for the weighted mean drift flow rate,

$$Uu_g^* = \hat{C}_0 U u^* + \hat{u}_b \tag{2.58}$$

$$u_g^* = \hat{C}_0 u^* + \hat{u}_b^*. \tag{2.59}$$

Since α is dimensionless, it is not scaled. It can however be expressed using either the actual flow rates or the scaled flow rates,

$$\alpha = \frac{Uu^*}{\hat{C}_0 U u^* + \hat{U} u_b^*} \tag{2.60}$$

$$= \frac{u^*}{\hat{C}_0 u^* + \hat{u}_b^*} \tag{2.61}$$

The star notation may be dropped to find the following set of dimensionless equations

$$\partial_t \rho + \partial_z(\rho u) = 0, \tag{2.62}$$

$$\rho\left(\partial_t u + u\partial_z u\right) + \partial_z p = -\rho\left(\frac{1}{Fr} + 2fu^2\right), \tag{2.63}$$

$$\rho = \alpha M^2 p + (1-\alpha). \tag{2.64}$$

2.4.1. SPECIAL CASES

The equations (2.62) and (2.63) hold in general, two-phase flow as well as single phase flow. In this section a couple of special cases are reviewed.

LAMINAR FLOW

The momentum equation for laminar flow (2.15) can also be written in dimensionless form. The variables in the Reynolds number must now be replaced using the dimensionless variables and the scaling values, $L = D$, U and R.

$$Re = \frac{R\rho U u D}{\mu} = Re_{ref}\rho u \tag{2.65}$$

$$f = \frac{16}{Re} = \frac{16}{Re_{ref}\rho u} \tag{2.66}$$

Then the dimensionless equations are the following,

$$\partial_t \rho + \partial_z(\rho u) = 0, \tag{2.67}$$

$$\rho\left(\partial_t u + u\partial_z u\right) + \partial_z p = -\left(\frac{\rho}{Fr} + \frac{32u}{Re_{ref}}\right). \tag{2.68}$$

This relation holds for all laminar flow regimes.

INCOMPRESSIBLE SINGLE PHASE FLOW

For single phase incompressible flow the density is constant in space as well as time. For this case the scaled ρ can be assumed equal to one, as in take $R = \rho$. Therefore

$$\partial_z u = 0, \tag{2.69}$$

$$\partial_t u + \partial_z p = -\left(\frac{1}{Fr} + 2fu^2\right). \tag{2.70}$$

Since the density ρ is known the system has gone from three to two unknowns. Aside form single phase incompressible flow there is also pseudo-incompressible flow. This is flow with a low Mach number, lets say $M^2 = \varepsilon$. In such cases by equation (2.64) the change of the density is of order $\mathcal{O}(\varepsilon)$. This means the change of density is small compared to the other variables and the density may be assumed constant. Then also the HEM equations (2.44) and (2.45) reduce to equations (2.69) and (2.70) respectively.

COMPRESSIBLE SINGLE PHASE FLOW

For single phase compressible flow the pressure is a function of the density, $p = p(\rho)$. Assuming an isothermal system and an ideal gas, the unscaled variables have the relation $p = c_g^2\rho$. Here c_g is the speed of sound in the gas. Taking $U = c_g$ gives the following relation between the dimensionless pressure and density, $p = \rho$. Then the dimensionless mass and momentum conservation equations become,

$$\partial_t p + \partial_z(pu) = 0, \tag{2.71}$$

$$p(\partial_t u + u\partial_z u) + \partial_z p = -p\left(\frac{1}{Fr} + 2fu^2\right). \tag{2.72}$$

Due to the closure relation between the pressure p and the density ρ, the number of unknown variables decreases to two. For two-phase flow the reference velocity U may also be set equal to the speed of sound c_g. This choice however effects the Froude number $Fr = \frac{U^2}{Lg}$ and the weight of the effect of the gravitational force $\frac{1}{Fr} \ll 1$. For the two-phase flow studied in this report a better choice would be to set U equal to the maximum flow rate of the IPR-curve as seen in section 1.2.

3

THE STEADY STATE SOLUTION

In this chapter the tubing performance relationship is considered in the context of the steady state setup of the problem. Different methods for finding the steady state solutions of equations (2.44) and (2.45) are given. These methods are discussed, compared and a choice will be made to plot the Tubing Performance Relationship curve.

3.1. TUBING PERFORMANCE RELATION CURVE

As explained in section 1.1, TPR curves plot the top site flow rate u_L against the pressure drop Δp over a given well, with a fixed top site pressure p_L. The TPR curve describes the flow conditions under steady state conditions. For this reason a closer look is taken at the steady state equations for the system, i.e. equations (2.44) and (2.45), derived in the previous chapter. Below the steady state versions of equations (2.44) and (2.45) are given with corresponding boundary conditions,

$$\partial_z(\rho u) = 0, \tag{3.1}$$

$$\rho u \partial_z u + \partial_z p = -\rho\left(\frac{1}{Fr} + 2fu^2\right), \tag{3.2}$$

$$\text{B.C.:} \quad u(L) = u_L \quad p(L) = p_L \tag{3.3}$$

By equation (3.1), $\rho u = C$, with C a nonnegative constant. Plugging this back into (3.2), results in

$$\partial_z p = -C\left(\frac{1}{uFr} + 2fu + \partial_z u\right), \quad \text{and by integration} \tag{3.4}$$

$$p(z) = -C\int_0^z \left\{\frac{1}{uFr} + 2fu + \partial_z u\right\} \mathrm{d}z + K_1. \tag{3.5}$$

With K_1 an integration constant. The parameters Fr and f are assumed constant and the integration constants C and K_1 can be deduced from the boundary conditions. However it is not clear how the flow rate u behaves as a function of z. Therefore equation (3.5) may not have an explicit analytic solution. Still, let us examen how the TPR curve can be derived using expression (3.5). The pressure increases with the depth of the well, thus decreases in the positive z-direction, and so the pressure drop over the well is given by,

$$\Delta p = p(0) - p(L). \tag{3.6}$$

Assuming the shape and value of the function $u(z)$ is dependent on the top site flow rate $u(L) = u_L$, then the pressure drop Δp can be expressed as a function of u_L,

$$\Delta p(u_L) = C(p_L, u_L)\int_0^L \left\{\frac{1}{u(z;u_L)Fr} + 2fu(z;u_L) + \partial_z u(z;u_L)\right\} \mathrm{d}z. \tag{3.7}$$

Note how the integration constant $C = \rho u$ is dependent on both the top site flow rate u_L as well as the top site pressure p_L. This is possible since there is a way to express the density ρ, in terms of flow rate and pressure, as shown in equation (2.55). In the next section this equation is used to express the steady state problem as a function of only the flow rate u and the pressure p. After which a numerical scheme is applied to solve further.

3.2. FULL NUMERICAL SOLUTION

To solve the steady state problem depicted by (3.1) and (3.2), a third relation between the variables u, ρ and p is required. This third relation is the expression for the mixture density ρ, i.e. the closure relation in equation (2.64), where α as defined in equation (2.61) is a function of the flow rate u. The idea is to use this expression for ρ repeated below,

$$\rho = \alpha(u)M^2 p + 1 - \alpha(u), \tag{3.8}$$

to rewrite $\partial_z \rho$ as a combination of $\partial_z u$ and $\partial_z p$. This results in the system below,

$$u\partial_p \rho \partial_z p + (u\partial_u \rho + \rho)\partial_z u = 0, \tag{3.9}$$

$$\rho u \partial_z u + \partial_z p = -\rho\left(\frac{1}{Fr} + 2fu^2\right). \tag{3.10}$$

It is then put in the following matrix form to facilitate computations,

$$\begin{pmatrix} u\partial_p \rho & u\partial_u \rho + \rho \\ 1 & \rho u \end{pmatrix} \partial_z \begin{pmatrix} p \\ u \end{pmatrix} = \begin{pmatrix} 0 \\ F(p,u) \end{pmatrix}. \tag{3.11}$$

Using a simple matrix inverse, an expression for $\partial_z p$ and for $\partial_z u$ is found

$$\partial_z p = \frac{-(u\partial_u \rho + \rho)}{u\partial_u \rho + \rho - \rho u^2 \partial_p \rho}\rho\left(\frac{1}{Fr} + 2fu^2\right), \tag{3.12}$$

$$\partial_z u = \frac{u\partial_p \rho}{u\partial_u \rho + \rho - \rho u^2 \partial_p \rho}\rho\left(\frac{1}{Fr} + 2fu^2\right). \tag{3.13}$$

The system of equations (3.12) and (3.13) is solved numerically with the help of maple™. Note that the Fanning friction factor f, the distribution correlation C_0 and the weighted mean drift velocity u_b depend on the flow regime, i.e. Reynolds number Re, and thus on u_L. The Reynolds number $Re = Re_{ref}\rho u$ (see equation (2.65)) and because of steady state conditions $\rho u = C$. Note that the Reynolds number is constant over the length of the pipe due to mass conservation and the assumption the mixture viscosity μ may be approximated by the liquid viscosity μ_l. A plot is made for C against the boundary condition u_L, i.e. figure 3.1. The Reynolds

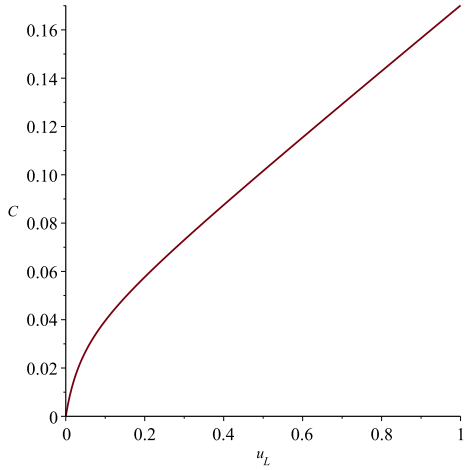

Figure 3.1: The TPR curve derived with a fully numerical scheme, with parameters $f = 0.005$, $Fr = 800$, $M^2 = 0.0025$, $C_0 = 1.155$ and $u_b = 0.05$

number is not the same for the different boundary conditions. As such the Fanning friction factor actually decreases as the flow rate increases. And the gas fraction α should be plotted in segments for each regime. For simplicity the parameters f, C_0 and u_b are kept constant. The resulting TPR curve shown below, while not a realistic representation of gas flow in a well, is a possible starting point for stability research. Given the forces on the flow and the gas-liquid mixture the TPR curve in figure 3.2 has the expected shape. For lower flow rates, there is a bigger liquid fraction and thus the gravitational force is bigger. For higher flow rates the liquid fraction and thus the gravitational force may be low but there will be a higher frictional force present. While the shape of the curve is as expected this fully numerical approach is not the only way to find the TPR curve. In the next section the solution for $\partial_z u$ is found numerically, after which this approximation is used in an exact expression for the pressure p.

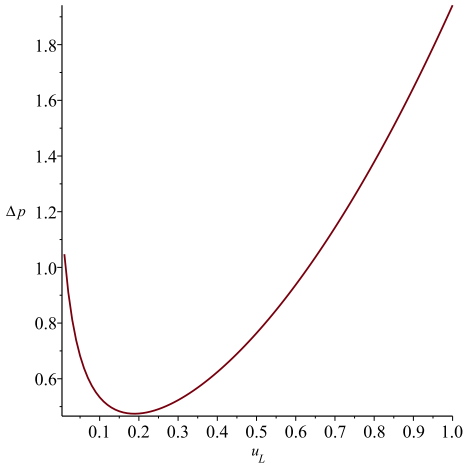

Figure 3.2: The TPR curve derived with a fully numerical scheme, with parameters $f = 0.005$, $Fr = 800$, $M^2 = 0.0025$, $C_0 = 1.155$ and $u_b = 0.05$

3.3. PARTIAL NUMERICAL SOLUTION

Starting from equation (3.4) and the relation $C = \rho u$, the pressure p can be expressed in terms of flow rate u using equation (3.8),

$$p = \frac{\rho - 1}{M^2 \alpha(u)} + \frac{1}{M^2} = \frac{C - u}{M^2 u \alpha(u)} + \frac{1}{M^2}. \tag{3.14}$$

Taking the derivative of equation (3.14) results in a second expression for $\partial_z p$, namely

$$\partial_z p = \frac{u^2 \alpha'(u) - C(u\alpha'(u) + \alpha)}{M^2 (u\alpha(u))^2} \partial_z u. \tag{3.15}$$

Combining equations (3.4) and (3.15), results in an expression for $\partial_z u$ that is only dependent on u,

$$\left(\frac{u^2 \alpha'(u) - C(u\alpha'(u) + \alpha)}{M^2 (u\alpha(u))^2} + C \right) \partial_z u = -C \left(\frac{1}{uFr} + 2fu \right), \tag{3.16}$$

$$\partial_z u = -C \frac{(1 + 2fu^2 Fr) M^2 (u\alpha(u))^2}{(u^2 \alpha'(u) - C(u\alpha'(u) + \alpha) + M^2 C (u\alpha(u))^2) uFr}. \tag{3.17}$$

With the help of the numerical solver of Maple™a solution for $u(z; u_L)$ can be derived. A plot is given for the bottom hole flow rate $u(0; u_L)$ given the top flow rate u_L. The bottom hole and top site flow rate are used in

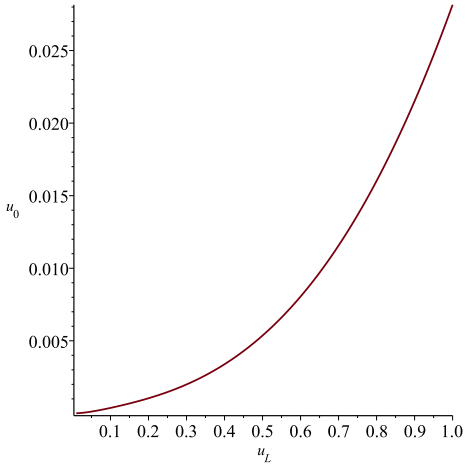

Figure 3.3: The bottom hole flow rate with parameters $f = 0.005$, $Fr = 800$, $M = 0.0025$, $C_0 = 1.155$ and $u_b = 0.05$

equation (3.14) in combination with (3.6),

$$\Delta p(u_L) = \frac{C(p_L, u_L) - u(0; u_L)}{M^2 u(0; u_L)\alpha(u(0; u_L))} - \frac{C(p_L, u_L) - u_L}{M^2 u_L \alpha(u_L)} \tag{3.18}$$

Let us call this way of finding the TPR curve a partially numerical scheme compared to the fully numerical scheme presented in the previous section 3.2. Comparing the full numerical scheme to the partially numer-

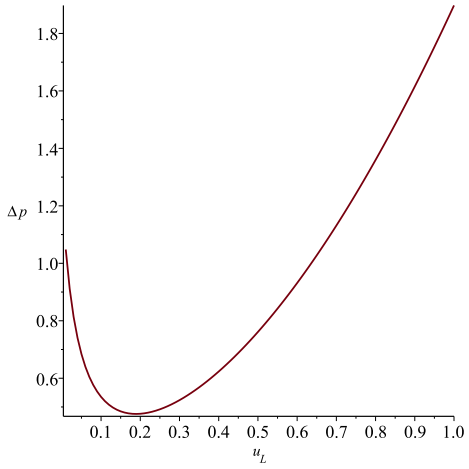

Figure 3.4: The TPR curve derived using a partially numeric scheme, with parameters $f = 0.005$, $Fr = 800$, $M^2 = 0.0025$, $C_0 = 1.155$ and $u_b = 0.05$

ical scheme in figure 3.5, a difference in pressure drop Δp is only noticeable for higher flow rates. Looking closer at the minimum of the curve there is almost no difference in both curves. This is interesting since the region of interest for further stability analysis in the next chapters is the region around the minimum. In the next section the last approach to finding the TPR curve is introduced with the assumption of pseudo-

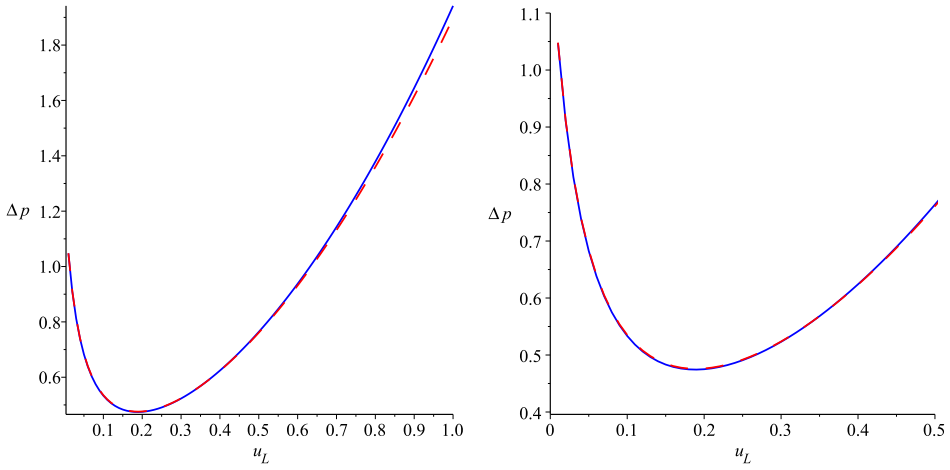

Figure 3.5: The TPR curves: full numeric in solid blue and partial numeric in dashed red, with parameters $f = 0.005$, $Fr = 800$, $M^2 = 0.0025$, $C_0 = 1.155$ and $u_b = 0.05$

incompressibility.

3.4. COMPRESSIBILITY ASSUMPTION

In practice it is assumed that $\partial_z u$ is close to zero. Taking a closer look at figure 3.3 this seems to hold for the lower flow rates. Comparing figure 3.3 to figure 3.4 for flow rates $u_L < 0.5$, the change of flow rate over the length of the pipe is about a hundred times smaller as the change in pressure over the pipe. To verify this, first the assumption is made that $\partial_z u \approx 0$ holds and then the TPR curve derived is compared to the TPR curves in the previous sections.

If indeed $\partial_z u \approx 0$ then looking at equation (3.13) the following must hold,

$$\frac{u\partial_p \rho}{u\partial_u \rho + \rho - \rho u^2 \partial_p \rho} \rho \left(\frac{1}{Fr} + 2fu^2 \right) \approx 0, \tag{3.19}$$

$$u\partial_p \rho \approx 0. \tag{3.20}$$

The above holds if $\partial_p \rho \approx 0$, by equation (3.8)

$$\partial_p \rho = \alpha(u) M^2. \tag{3.21}$$

Since $0 \leq \alpha \leq 1$, the approximation in Equation (3.20) is valid for small Mach numbers. The parameter $M = \frac{U}{c_g}$ is only a reference number Mach number. However since $U = u_{max}$ is equal to the maximum possible flow rate, M is an upper bound of the actual Mach number. Flows with $M < 0.2$ are called pseudo-incompressible, for these types of flow the mixture is indeed considered as incompressible. Mathematically this translates to solving the dominant, order $\mathcal{O}(1)$ system. Assuming Equation (3.20) holds, equations (3.12) and (3.13) can reduce to,

$$\partial_z p = \rho \left(\frac{1}{Fr} + 2fu^2 \right), \tag{3.22}$$

$$\partial_z u = 0. \tag{3.23}$$

The boundary condition $p(L) = p_L$ can be translated to ρ, where

$$\rho(L) = \alpha(u_L) M^2 p_L + 1 - \alpha(u_L). \tag{3.24}$$

The boundary condition for ρ has a order $\mathcal{O}(1)$ component and a order $\mathcal{O}(M^2)$ component. Thus to describe the full order $\mathcal{O}(1)$ problem the corresponding boundary conditions are $p(L) = 0$ and $u(L) = u_L$. With equations (3.22) and (3.23) an explicit analytic expressing can be derived for the pressure drop $\Delta p(u_L)$,

$$\Delta p(u_L) = (1 - \alpha(u_L)) \left(\frac{1}{Fr} + 2fu_L^2 \right) L. \tag{3.25}$$

The TPR curve for equation (3.25) is given in figure 3.6 and shows a similar form to the numerically found curves from the previous sections. Again as seen in figure 3.7 the difference is only visible for higher flow rates, where the curve lies between both numerical curves. Around the minimum of the curves, there is almost no distinguishable difference between the three curves. There are three reasons that this last approximation for the TPC curve is chosen for further analysis.

- Firstly, there is no need for a numerical solver.
- Secondly, assuming $\partial_z u = 0$ greatly simplifies the linearization done in chapter 5.
- And lastly, this version of the TPC curve has an explicit expression for the tangent of the TPR curve, $\partial_{u_L} \Delta p$.

In the next chapter a closer look is taken at nodel analysis and how it explains the stability criteria of the TPR curve.

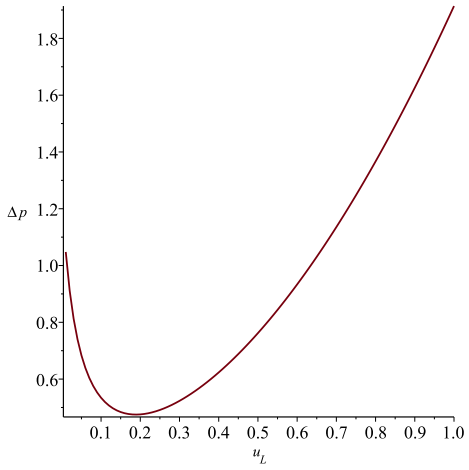

Figure 3.6: The TPR curve derived using pseudo-compressibility, with parameters $f = 0.005$, $Fr = 800$, $M^2 = 0.0025$, $C_0 = 1.155$ and $u_b = 0.05$

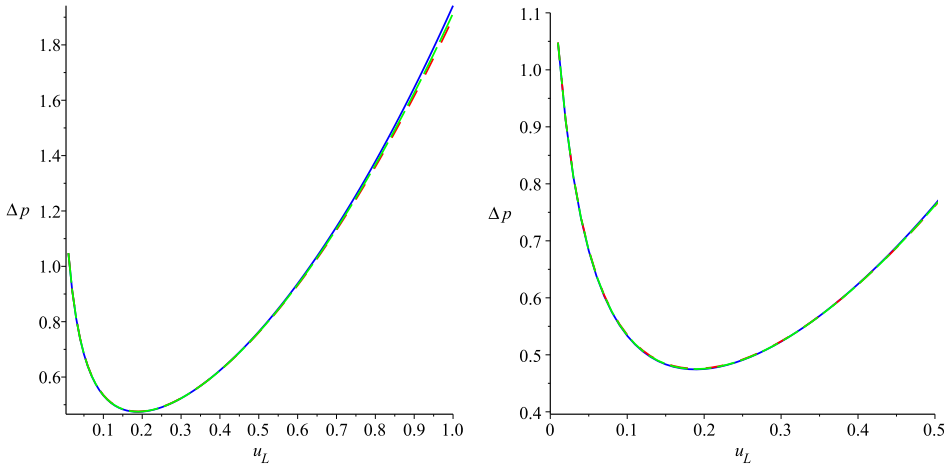

Figure 3.7: The TPR curves: full numeric in solid blue, partial numeric in dashed red and pseudo-compressible in dashed green, with parameters $f = 0.005$, $Fr = 800$, $M^2 = 0.0025$, $C_0 = 1.155$ and $u_b = 0.05$

4

THE FIXED POINT METHOD

The general way to determine the stability of any point on the tubing performance relation (TPR) curve, comes from nodal analysis. This chapter will first introduce nodal analysis and the stability region of the TPR curve. Then the stability argument from nodal analysis is compared to the fixed point method. Finally an alternative method of stability analysis using time dependency is shown and how this challenges traditional claims on the stable region of the TPR curve.

4.1. NODAL ANALYSIS

The production of gas from reservoir up to distribution pipeline can be described as a network of elements, i.e. figure 4.1. The nodes are the connections between each element. Each element has an inflow and an outflow node. For each element there is a relation between the inflow variables and the outflow variables.

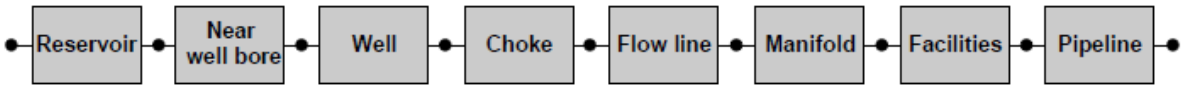

Figure 4.1: A simplified schematic production system from [3]

For example the pressure p and the flow rate u at the outflow node may be expressed as a function of these variables at the inflow node, i.e.

$$p_{out} = f(p_{in}, u_{in}), \tag{4.1}$$
$$u_{out} = g(p_{in}, u_{in}). \tag{4.2}$$

Generally the functions f and g can not be described as explicit analytic functions and are approximated numerically. There are two ways nodal analysis is used to predict the unknown variables at a node, where this node is called the analysis node. Using the inflow-outflow relation of each element the unknown variables at the analysis node can be determined using the variables at a different node either downstream or upstream of the analysis node.
The second approach is, to use both a node downstream as well as a node upstream of the analysis node, as shown in figure 4.2. For both sides of the analysis node an estimate is made and these are compared to find ideal production conditions. This approach is applied to the bottom hole node.
Essentially the TPR curve gives the inflow-outflow relation of the well element. And the inflow performance relation (IPR) curve introduced in section 1.2 gives this relation for the reservoir element. Now the inflow node of the well coincides with the outflow node of the reservoir. As such the TPR curve and the IPR curve show the nodal analysis for this node, i.e. the bottom hole node.
Any intersection of the TPR curve and the IPR curve is called a natural production point. If a small perturbation to the natural production conditions adjusts back to the original production conditions over time it is called stable.

Definition 4.1 (Stable production point)**.** Given the vector $\mathbf{v}_0$ of variables describing the natural production point and the perturbation vector $\delta\mathbf{v}$ of which at least one element is nonzero then,

$$\lim_{t\to\infty} \mathbf{v}_0 + \delta\mathbf{v} \to \mathbf{v}_0. \tag{4.3}$$

If a production point is not stable it is called unstable.

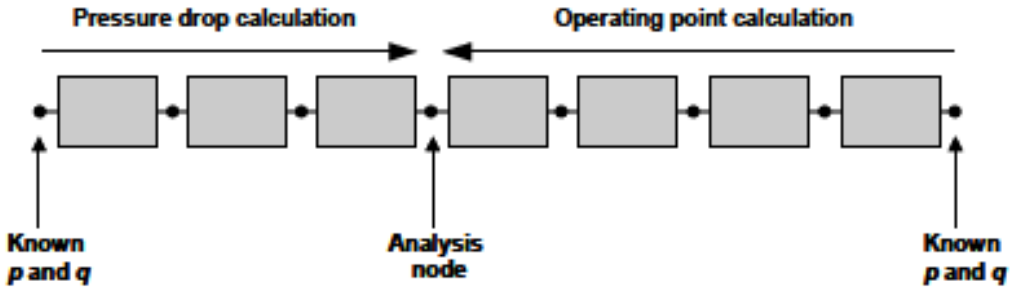

Figure 4.2: A schematic production system with two side nodal analysis from [3]

Now the idea propagating in books like [2] and others is that the perturbation happens along the IPR curve. After which the pressure in the well adjusts according to the new flow rate. Then the flow from the reservoir will react to the new pressure and so on. This approach always results in instability for production points to the left of the minimum of the TPR curve. This step wise adjustment scheme is a discrete approach to

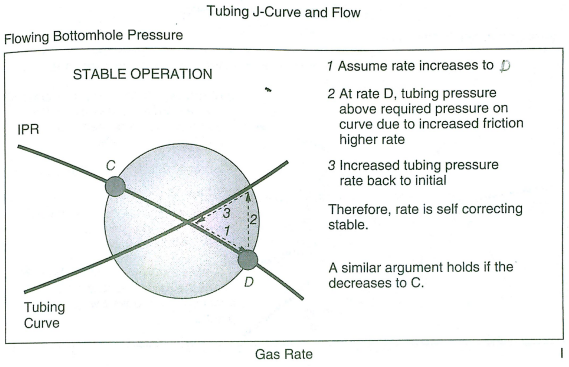

(a) Stable from [2]

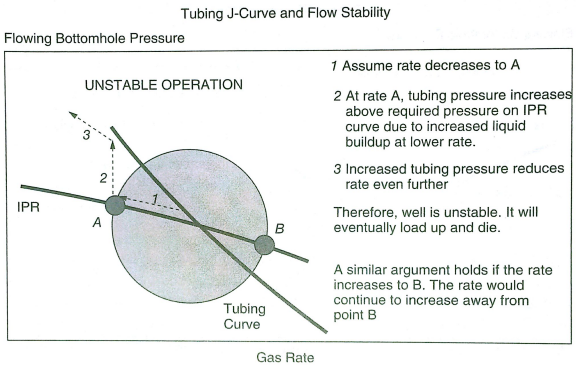

(b) Unstable from [2]

analysing a continuous process. The main problem with this scheme is that the choice to first adjust the pressure over the well is not mathematically motivated. And an adjustment in flow rate over the well followed by an adjustment in pressure over the reservoir result in different conclusions about the stability of a production point. It can be observed that this step wise scheme is equivalent to the fixed point algorithm for finding intersections of two curves. And unless the derivatives of the curves are zero this scheme can always converge given the right criteria. The next section will explain the fixed point algorithm further and connect it with the stability analysis of the TPR and IPR curve.

4.2. FIXED POINT ALGORITHM

A fixed point iteration can help approximate the solution to the equation $x = h(x)$. Given the initial guess x_0 of the solution a, $a = h(a)$, the algorithm calculates $x_{n+1} = h(x_n)$ for $n = 1, 2, \ldots, N$. Where N is dependent on a predetermined error bound ϵ.

Algorithm 1 Fixed point iteration

Initial guess x_0,
$r_0 = \epsilon + 1$, $i = 0$
while $r_i > \epsilon$ **do**
  $x_{i+1} \leftarrow h(x_i)$
  $r_{i+1} \leftarrow |x_{i+1} - x_i|$
  $i \leftarrow i + 1$
end while

Taylor expansion is used to show under which conditions the algorithm works.

$$x_1 = h(x_0) \tag{4.4}$$
$$= a + h'(a)(x_0 - a) + \mathcal{O}((x_0 - a)^2) \tag{4.5}$$
$$x_2 = h(x_1) \tag{4.6}$$
$$= a + h'(a)^2(x_0 - a) + \mathcal{O}((x_0 - a)^2) \tag{4.7}$$
$$x_{n+1} = h(x_n) \tag{4.8}$$
$$\approx a + h'(a)^n(x_0 - a). \tag{4.9}$$

So for a good initial guess x_0 close to a the limit of x_n will be

$$\lim_{n\to\infty} x_n = a + (x_0 - a) \lim_{n\to\infty} h'(a)^n \tag{4.10}$$

If $|h'(a)| < 1$ the sequence x_n converges asymptotically to a.

This algorithm can also be used to find the intersection of two functions $f(x)$ and $g(x)$. To solve the equation $f(x) = g(x)$ it first needs to be rewritten in the form $x = h(x)$. One way of doing this is by using the inverse function,

$$f(x) = g(x), \tag{4.11}$$
$$x = f^{-1}(g(x)). \tag{4.12}$$

To see if the choice $h(x) = f^{-1}(g(x))$ is stable the derivative is determined in a, where $f(a) = g(a)$,

$$h'(a) = \frac{1}{f'(f^{-1}(g(a)))} g'(a), \tag{4.13}$$
$$= \frac{g'(a)}{f'(f^{-1}(f(a)))}, \tag{4.14}$$
$$= \frac{g'(a)}{f'(a)}. \tag{4.15}$$

Now if it turns out $|h'(a)| > 1$ then the following choice will guarantee convergence,

$$h(x) = g^{-1}(f(x)), \tag{4.16}$$
$$h'(a) = \frac{f'(a)}{g'(a)} \tag{4.17}$$

This choice for $h(x)$ will definitely converge.

For the TPR and IPR curves this means going back to the steady state production point is a question of choosing wether the pressure or the flow rate will adjust itself first. The literature studied only gives an intuitive argument, as to why the well and reservoir would react in that manner. The goal of this thesis is to verify the claim of stability to the left of the minimum of the TPR curve mathematically. The next section shows an alternative approach to nodal analysis which shows a possible stable region slightly left of the minimum of the TPR curve, and thus expanding on the original claims of a stable region.

4.3. ALTERNATIVE METHOD IN NODAL ANALYSIS

Assuming the functions for the TPR and IPR curves exist set, $f(u) = p_{IPR}$ and $g(u) = p_{TPR}$. Now f returns the bottom hole pressure for the reservoir given flow rate u and g returns the bottom hole pressure for the well given flow rate u. Now let us assume the flow rate has been perturbed with new flow rate $u + \delta u$. Then using a Taylor expansion a prediction of the perturbation δp in the pressure can be given for both f and g.

$$\delta p_f = f'\delta u \quad \text{and} \quad \delta p_g = g'\delta u \tag{4.18}$$

Note however that $\delta p_f \neq \delta p_g$, this is because the time dependency is not taken into account. In [3] the actual acceleration needed to go from u to $u+\delta u$ deemed the cause for extra pressure fluctuations. An inertial term is then added to both equations,

$$\delta p_f = f'\delta u - \hat{f}\partial_t u \quad \text{and} \quad \delta p_g = g'\delta u + \hat{g}\partial_t u. \tag{4.19}$$

Both the constants $\hat{f}$ and $\hat{g}$ are positive. As an increase of pressure at the node causes an acceleration downstream and an deceleration upstream. To understand this effect, imagine the increase of pressure as a small explosion at a fixed point propagating through a moving medium. Assuming that $\delta p_f = \delta p_g$ holds, the flow rate perturbation can be described as a function of time,

$$f'\delta u - \hat{f}\partial_t \delta u = g'\delta u + \hat{g}\partial_t \delta u, \tag{4.20}$$

$$(\hat{f} + \hat{g})\partial_t \delta u = (f' - g')\delta u, \tag{4.21}$$

$$\delta u = C\exp\left(\frac{f' - g'}{\hat{f} + \hat{g}}\, t\right). \tag{4.22}$$

The stable region of flow rate u with perturbation δu as given by definition 4.1 is the flow rates u for which $f' - g' < 0$. Thus the stability of the perturbation is dependent on the difference in slope between the IPR and TPR curves. In [13] there is another argument made to look at the slope of the combined curve $f - g$ in stead of the slope of the TPR curve only. The curve $f - g$ is essentially combining two segments in the nodal analysis and treating it as one. Also note that due to the decreasing shape of the IPR curve the minimum of the combined curve will always lie to the left of the minimum of the TPR curve. This area between both minima is assumed to extend the stability region of the TPR curve. In the next chapter the time behaviour of perturbations are studied. First the original stability region will be confirmed, after which a possible extension of the region is discussed.

5

A STUDY ON TIME DEPENDENCE

In this chapter the transient, i.e. the time dependent, system is studied. This is done by adding a small perturbation to the steady state solution and studying how this perturbation behaves in time.

5.1. TAYLOR LINEARIZATION

Any nonlinear (and *sufficiently* smooth) function may be linearized at any point using its Taylor expansion. For small deviations from the point of linearization this provides a good approximation. A time derivative of the form $\dot{x} = f(x)$, where f(x) is a nonlinear function of x can be linearized around its steady state point. This technique is used for stability analysis, for instructions and examples see Verhulst [14]. The idea is to rewrite the system of equations (2.44) and (2.45) in matrix form with the help of the relation $\rho = \rho(p,u)$,

$$\begin{pmatrix} \partial_p\rho & \partial_u\rho \\ 0 & \rho \end{pmatrix}\partial_t\begin{pmatrix} p \\ u \end{pmatrix} + \begin{pmatrix} u\partial_p\rho & u\partial_u\rho+\rho \\ 1 & \rho u \end{pmatrix}\partial_z\begin{pmatrix} p \\ u \end{pmatrix} + \begin{pmatrix} 0 \\ \rho\left(\frac{1}{Fr}+2fu^2\right) \end{pmatrix} = \mathbf{0}. \tag{5.1}$$

The vector of unknown variables is called $\mathbf{v}$ and the matrices are called A, B and R respectively. Then equation (5.1) is rewritten to find a expression for the time derivative $\partial_t\mathbf{v}$,

$$A\partial_t\mathbf{v} + B\partial_z\mathbf{v} + R = \mathbf{0}, \tag{5.2}$$

$$\partial_t\mathbf{v} + A^{-1}B\partial_z\mathbf{v} + A^{-1}R = \mathbf{0}, \tag{5.3}$$

$$\partial_t\mathbf{v} = -\left(A^{-1}B\partial_z\mathbf{v} + A^{-1}R\right). \tag{5.4}$$

Note for $\rho > 0$ and $u > 0$ the matrix A is nonsingular since $\partial_p\rho = \alpha M^2$. Now the time derivative is of the form $\partial_t\mathbf{v} = F(\mathbf{v})$, however F is not a nonlinear function but a nonlinear operator (see Definition A.1). For an operator $F(\mathbf{v}) : V \to W$ the Taylor expansion at $\mathbf{v}_0$ is given by,

$$F(\mathbf{v}) = F(\mathbf{v}_0) + \left.\frac{\partial F}{\partial \mathbf{v}}\right|_{(\mathbf{v}_0)}(\mathbf{v}-\mathbf{v}_0) + \mathcal{O}(\|\mathbf{v}-\mathbf{v}_0\|^2).$$

However, since F is an operator on an element $\mathbf{v} \in V$, taking a derivative with respect to $\mathbf{v}$ is not a straight forward process. Refer to definition A.2 and A.3 for the generalization of the derivative and the directional derivative respectively, as they are known in general calculus. If the Gâteaux derivative A.3 of f is linear in $\mathbf{h}$, i.e. of the form $\mathrm{d}_h f(x) = A_x\mathbf{h}$, then the Fréchet derivative A.2 of f is $Df(x) = A_x$.

To calculate the Gâteaux derivative first define,

$$F(\mathbf{v}_0 + t\mathbf{h}) = -(A^{-1}B)|_{\mathbf{v}_0+t\mathbf{h}}(\mathbf{v}_0 + t\mathbf{h})_z - (A^{-1}R)|_{\mathbf{v}_0+t\mathbf{h}} \tag{5.5}$$

$$= -\left[(A^{-1}B)|_{\mathbf{v}_0} + (A^{-1}B)'|_{\mathbf{v}_0} t\mathbf{h}\right][(\mathbf{v}_0)_z + t\mathbf{h}_z] + \\ -(A^{-1}R)|_{\mathbf{v}_0} - (A^{-1}R)'|_{\mathbf{v}_0} t\mathbf{h} + \mathcal{O}(t^2\mathbf{h}^2), \tag{5.6}$$

$$= -(A^{-1}B)|_{\mathbf{v}_0}(\mathbf{v}_0)_z - (A^{-1}R)|_{\mathbf{v}_0} + \\ -(A^{-1}B)|_{\mathbf{v}_0} t\mathbf{h}_z - (A^{-1}R)'|_{\mathbf{v}_0} t\mathbf{h} + \\ -(A^{-1}B)'|_{\mathbf{v}_0} t\mathbf{h}(\mathbf{v}_0)_z + \mathcal{O}(t^2), \tag{5.7}$$

$$= F(\mathbf{v}_0) + \\ -t\left[(A^{-1}B)|_{\mathbf{v}_0}\mathbf{h}_z + (A^{-1}R)'|_{\mathbf{v}_0}\mathbf{h} + (A^{-1}B)'|_{\mathbf{v}_0}\mathbf{h}(\mathbf{v}_0)_z\right] + \mathcal{O}(t^2). \tag{5.8}$$

Where A' is the derivative of A with respect to $\mathbf{v}$. The Gâteaux derivative of $F(\mathbf{v})$ is

$$\mathrm{d}_{\mathbf{h}}F(\mathbf{v}_0) = \lim_{t\to 0}\frac{F(\mathbf{v}_0 + t\mathbf{h}) - F(\mathbf{v}_0)}{t} \tag{5.9}$$

$$= -\left((A^{-1}B)|_{\mathbf{v}_0}\partial_z + (A^{-1}R)'|_{\mathbf{v}_0} + (A^{-1}B)'|_{\mathbf{v}_0}(\mathbf{v}_0)_z\right)\mathbf{h} \tag{5.10}$$

$$= \left(\bar{B}|_{\mathbf{v}_0}\partial_z + \bar{R}|_{\mathbf{v}_0}\right)\mathbf{h} \tag{5.11}$$

And equivalently the Fréchet derivative is $DF(\mathbf{v}_0) = \bar{B}|_{\mathbf{v}_0}\partial_z + \bar{R}|_{\mathbf{v}_0}$, interchanging the operator derivative with the Fréchet derivative define

$$\left.\frac{\partial F}{\partial \mathbf{v}}\right|_{(\mathbf{v}_0)} = DF(\mathbf{v}_0) \tag{5.12}$$

Since $\mathbf{v}_0$ was chosen such that $F(\mathbf{v}_0) = 0$, the Taylor expansion around $\mathbf{v}_0$ is given by

$$F(\mathbf{v}) = DF(\mathbf{v}_0)(\mathbf{v} - \mathbf{v}_0). \tag{5.13}$$

The eigenvalues ω of the linearized operator F can be found, setting $\delta\mathbf{v} = \mathbf{v} - \mathbf{v}_0$,

$$(\bar{B}\partial_z + \bar{R})\delta\mathbf{v} = \omega\delta\mathbf{v}, \tag{5.14}$$

$$\bar{B}\partial_z\delta\mathbf{v} = (\omega I - \bar{R})\delta\mathbf{v}, \tag{5.15}$$

$$\partial_z\delta\mathbf{v} = \bar{B}^{-1}(\omega I - \bar{R})\delta\mathbf{v}, \tag{5.16}$$

$$= C(\omega)\delta\mathbf{v}. \tag{5.17}$$

Equation (5.17) has the solution $\delta\mathbf{v} = \mathbf{K}_1\exp(C(\omega)z)$. Define the eigenvalues κ of $C(\omega)$, then

$$\omega\delta\mathbf{v} = (\bar{B}\kappa + \bar{R})\delta\mathbf{v} \tag{5.18}$$

Equation (5.18) can be solved for ω, by setting the determinant to zero. The determinant is one equation of two unknowns, ω and κ. The steady state solution $\mathbf{v}_0$ is stable if all eigenvalues $\omega \le 0$ and asymptotically stable if all eigenvalues $\omega < 0$. However without knowing κ, the sign of ω can only be determined if the vector $\delta\mathbf{v}$ is known. Since a general description, regardless of $\delta\mathbf{v}$, is desired, the Taylor linearization by itself is apparently not enough to determine a stability region. The next section will approach the linearization of the problem in a different context.

5.2. TRANSFER FUNCTION

In this section the perturbations behaviour on the frequency domain is studied to produce a transfer function. To move from the time domain to the frequency domain a fourier transform is applied. The fourier transform of a function $f(t)$ is

$$\hat{f}(\omega) = \int_{\infty}^{\infty} f(t)e^{-i\omega t}\,\mathrm{d}t. \tag{5.19}$$

The nice thing about the Fourier transform is that a derivative on the time domain is equivalent to a multiplication on the frequency domain,

$$\widehat{\partial_t f}(\omega) = i\omega\hat{f}(\omega). \tag{5.20}$$

Before moving to the frequency domain let us define the unknown variables using the steady state solution and a time dependent perturbation,

$$p = \bar{p}(z) + \delta p(z,t),$$
$$u = \bar{u}(z) + \delta u(z,t).$$

The time dependent perturbations δp and δu are assumed small compared to the steady state variables. The density ρ can also be expressed with a time-dependent part $\delta\rho$ and a steady state part $\bar{\rho}$,

$$\rho(p,u) = \rho(\bar{p},\bar{u}) + \partial_p\rho\delta p + \partial_u\rho\delta u, \tag{5.21}$$
$$= \bar{\rho}(z) + \delta\rho(z,t). \tag{5.22}$$

Plugging these into equations (2.44) and (2.45), repeated below,

$$\partial_t\rho + \partial_z(\rho u) = 0, \tag{5.23}$$
$$\rho\left(\partial_t u + u\partial_z u\right) + \partial_z p + \rho\left(\frac{1}{Fr} + 2fu^2\right) = 0. \tag{5.24}$$

The steady state relation below holds,

$$\partial_z(\bar{\rho}\bar{u}) = 0, \tag{5.25}$$
$$\bar{\rho}\bar{u}\partial_z\bar{u} + \partial_z\bar{p} + \bar{\rho}\left(\frac{1}{Fr} + 2f\bar{u}^2\right) = 0. \tag{5.26}$$

So taking the difference of equations (5.23) and (5.24) with equations (5.25) and (5.26) respectively, results in a set of differential equations for the perturbations δp, δu and $\delta\rho$,

$$\partial_t\delta\rho + \partial_z(\bar{\rho}\delta u + \bar{u}\delta\rho) = 0 \tag{5.27}$$
$$\bar{\rho}\left(\partial_t\delta u + \partial_z(\bar{u}\delta u)\right) + \delta\rho\bar{u}\partial_z\bar{u} + \partial_z\delta p + \left(\frac{1}{Fr} + 2f\bar{u}^2\right)\delta\rho + 4f\bar{u}\delta u = 0 \tag{5.28}$$

Note any quadratic terms in perturbation values have been removed. Now to perform the Fourier transform, the perturbations become,

$$\delta p \to \hat{P}(z,\omega), \tag{5.29}$$
$$\delta u \to \hat{U}(z,\omega), \tag{5.30}$$
$$\delta\rho \to \hat{R}(z,\omega) = \partial_p\rho\hat{P}(z,\omega) + \partial_u\rho\hat{U}(z,\omega), \tag{5.31}$$

and the differential equations (5.27) and (5.28) become

$$i\omega\hat{R} + \partial_z(\bar{\rho}\hat{U} + \bar{u}\hat{R}) = 0, \tag{5.32}$$
$$\bar{\rho}\left(i\omega\hat{U} + \partial_z(\bar{u}\hat{U})\right) + \hat{R}\bar{u}\partial_z\bar{u} + \partial_z\hat{P} + \left(\frac{1}{Fr} + 2f\bar{u}^2\right)\hat{R} + 4f\bar{u}\hat{U} = 0. \tag{5.33}$$

Replacing $\hat{R}$ according to equation (5.31) gives equivalent relations as (5.17) or (5.18). This becomes especially apparent if another Fourier transformation is applied,

$$\hat{P}(z,\omega) \to P(\kappa,\omega), \tag{5.34}$$
$$\hat{U}(z,\omega) \to U(\kappa,\omega). \tag{5.35}$$

This gives a very long expression with several derivatives which is equivalent to (5.18),

$$i\omega(\partial_p\rho P + \partial_u\rho U) + i\kappa(\bar{\rho}U + \bar{u}(\partial_p\rho P + \partial_u\rho U)) + U\partial_z\bar{\rho} + (\partial_p\rho P + \partial_u\rho U)\partial_z\bar{u} = 0, \tag{5.36}$$
$$\bar{\rho}\left(i\omega U + U\partial_z(\bar{u}) + \bar{u}i\kappa U\right) + (\partial_p\rho P + \partial_u\rho U)\bar{u}\partial_z\bar{u} + i\kappa P + \left(\frac{1}{Fr} + 2f\bar{u}^2\right)(\partial_p\rho P + \partial_u\rho U) + 4f\bar{u}U = 0. \tag{5.37}$$

The actual transfer function can be derived from equations (5.36) and (5.37), see chapter 15 of [13] for instructions. The transfer function will have the form

$$\begin{pmatrix} P_2 \\ U_2 \end{pmatrix} = T(z_2 - z_1)\begin{pmatrix} P_1 \\ U_1 \end{pmatrix}. \tag{5.38}$$

This expression is especially useful for nodal analysis, κ can then be estimated if data is collected from two locations along the flow. Once κ is determined, ω can be derived. This approach while interesting is not worked out further because it is more suited for practical uses as apposed to analyses of a general problem.

5.2.1. PSEUDO-COMPRESSIBILITY

The linearized equations derived in the previous and this section are very long and have several derivatives. It is to easy lose oversight of the situation and the possible weight and sign of the constants. For this reason, the pseudo-compressibility introduced in section 3.4 is also applied to the time dependent part of the problem. This means that $\partial_p \rho \approx 0$ and terms containing this derivatives are adjusted as if equality holds. Resulting in equation (5.36) and (5.37) being condensed to,

$$(i\omega + \bar{u} i\kappa)\partial_u \rho + \bar{\rho} i\kappa = 0, \tag{5.39}$$

$$(\bar{\rho}(i\omega + \bar{u} i\kappa) + \partial_u F(\bar{u}))U + i\kappa P = 0. \tag{5.40}$$

With $F(\bar{u}) = (1-\alpha(\bar{u}))\left(\frac{1}{Fr} + 2f\bar{u}^2\right)$. This linearization gives a better overview. In the next section some choices for the initial perturbation are discussed, to study if this choice effects the time dependancy.

5.3. PROJECTION OF THE INITIAL PERTURBATIONS

Instead of defining κ assume the initial perturbation is known and can be projected onto a basis vector. Then for each basis vector a value for ω can be derived. The first basis to look at, are the unit vectors in the p and u direction, $(1,0)^T$ and $(0,1)^T$. For

$$\begin{pmatrix} P \\ U \end{pmatrix} = \begin{pmatrix} 0 \\ 1 \end{pmatrix} U, \tag{5.41}$$

equations (5.39) and (5.40) can be rewritten as

$$(i\omega + \bar{u} i\kappa)\partial_u \rho + \bar{\rho} i\kappa = 0, \tag{5.42}$$

$$\bar{\rho}(i\omega + \bar{u} i\kappa) + \partial_u F(\bar{u}) = 0. \tag{5.43}$$

This gives the following expression for $i\omega$,

$$i\omega = -\partial_u F \frac{\partial_u \rho + \bar{\rho}}{\bar{\rho}^2}. \tag{5.44}$$

Before determining the sign of this $i\omega$ a look is taken at the second projection basis. This choice of basis provides little information on the second $i\omega$, since the second base vector eliminates ω completely from equations (5.39) and (5.40). A better choice is to project the perturbation onto the tangent and the normal of the TPR curve. The tangential and normal basis vectors are of the form,

$$\begin{pmatrix} P \\ U \end{pmatrix} = \begin{pmatrix} \partial_u p \\ 1 \end{pmatrix} U, \quad \text{and} \quad \begin{pmatrix} P \\ U \end{pmatrix} = \begin{pmatrix} 1 \\ -\partial_u p \end{pmatrix} P. \tag{5.45}$$

The basis vectors are put into (5.39) and (5.40) to find two sets of relations for $i\omega$,

Tangential relations:

$$(i\omega + \bar{u} i\kappa)\partial_u \rho + \bar{\rho} i\kappa = 0, \tag{5.46}$$

$$\bar{\rho}(i\omega + \bar{u} i\kappa) + \partial_u F(\bar{u}) + i\kappa \partial_u p = 0, \tag{5.47}$$

Normal relations:

$$(i\omega + \bar{u} i\kappa)\partial_u \rho + \bar{\rho} i\kappa = 0, \tag{5.48}$$

$$(\bar{\rho}(i\omega + \bar{u} i\kappa) + \partial_u F(\bar{u}))\partial_u p - i\kappa = 0. \tag{5.49}$$

Using these equations the following values for $i\omega_{tan}$ and $i\omega_{norm}$ are derived,

$$i\omega_{tan} = -\partial_u F \frac{\bar{u}\partial_u \rho + \bar{\rho}}{\bar{\rho}^2 - \partial_u p \partial_u \rho}, \tag{5.50}$$

$$i\omega_{norm} = -\partial_u F \frac{\bar{u}\partial_u \rho + \bar{\rho}}{\bar{\rho}^2 + \frac{\partial_u \rho}{\partial_u p}}. \tag{5.51}$$

Looking at the TPR curve derived with the psuedo-compressibility assumption, i.e. equation (3.25), its derivative with respect to u_L equals,

$$\partial_{u_L} \Delta p = L \partial_u F. \tag{5.52}$$

So the sign of $\partial_u F$ changes along with the tangent of the TPR curve. So to study the stability a look is taken at the fractions in (5.50) and (5.51). Their numerator is given below using the relation (3.24) with the corresponding boundary conditions,

$$\bar{u}\partial_u \rho + \bar{\rho} = 1 - \alpha(\bar{u}) - \bar{u}\partial_u \alpha(\bar{u}). \tag{5.53}$$

Due to the fact that $C_0 \geq 1$ the numerator (5.53) has positive values for all flow rates $\bar{u}$. This is show graphicly in figure 5.1. Now to look at each denominator, for (5.51) the denominator is

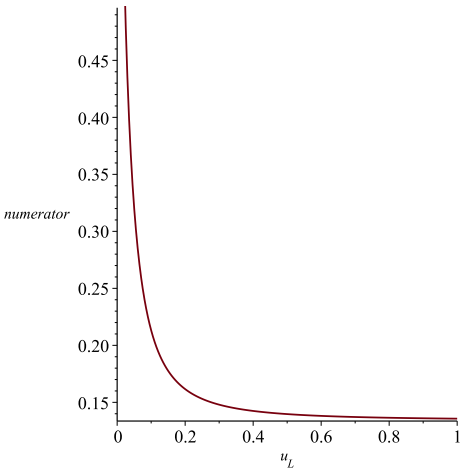

Figure 5.1: The numerator for different steady state values

$$\bar{\rho}^2 + \frac{\partial_u \rho}{\partial_u p} = \bar{\rho}^2 + \partial_p \rho. \tag{5.54}$$

Since $\partial_p \rho \geq 0$ for all flow rates, the perpendicular component is only stable, i.e. $i\omega_{norm} < 0$, if $\partial_u F > 0$. Thus the normal component is only stable to the right of the TPR curve. For (5.50) again use relation (3.24) to derive the denominator

$$\bar{\rho}^2 - \partial_u p \partial_u \rho = \bar{\rho}^2 + \partial_u \alpha \partial_u p. \tag{5.55}$$

Because $\partial_u \alpha > 0$, the tangential component is certainly stable to the right of the TPR curve. However if there are values of $\partial_u p < 0$ for which expression (5.55) is negative, then the region of stability for the tangential component is slightly bigger. In the overall picture this does not matter, since both the eigenvalues (denoted by $i\omega$) need to be non-positive for stability.

Other projections could be tested to confirm the stability. However since the same perturbation gets projected on different bases the expectation is similar behavior. Either no conclusion can be made as in the first case or the same conclusion is made. The production points on the TPR curve that are to the left of its minimum are indeed stable.

5.3.1. BACK TO NODAL ANALYSIS

In chapter 4 the last section shows the possibility of stable production points to the left of the minimum of the TPR curve. For this reason another look is taken at that approach. According to equation (4.19) a perturbation would behave as follows

$$\delta p_g = g' \delta u + \hat{g} \partial_t u \tag{5.56}$$

Where the function g would be equivalent the bottom hole pressure given by $p_L + \Delta p$, where Δp is defined in equation (3.7), so to repeat

$$g = p(L) + \Delta p(u_L) = p_L + C(p_L, u_L) \int_0^L \left\{ \frac{1}{u(z;u_L)Fr} + 2f u(z;u_L) + \partial_z u(z;u_L) \right\} \mathrm{d}z. \tag{5.57}$$

If equation g was derived without the steady state assumption then

$$g_t = p_L + C(p_L, u_L)\int_0^L \left\{ \frac{1}{u(z;u_L)Fr} + 2f\,u(z;u_L) + \partial_z u(z;u_L) + \frac{1}{u(z;u_L)}\partial_t u(z;u_L) \right\} \mathrm{d}z, \tag{5.58}$$

$$g_t = g + \int_0^L \rho(z;p_L,u_L)\partial_t u(z;u_L)\,\mathrm{d}z. \tag{5.59}$$

For steady state conditions $g_t = g$ then if these conditions are perturbed and the perturbation is time dependent then

$$g_t(u+\delta u) = g + g'\delta u + \int_0^L \rho(z;p_L,u_L)\partial_t \delta u\,\mathrm{d}z \tag{5.60}$$

Now if $\delta u = \phi(z)\psi(t)$ then

$$g_t - g = g'\delta u + \hat{g}\delta u \qquad \text{with,} \tag{5.61}$$

$$\hat{g} = \frac{1}{\phi(z)}\int_0^L \rho(z;p_L,u_L)\phi(z)\,\mathrm{d}z \tag{5.62}$$

Since $\rho > 0$ by definition, $\hat{g}$ will be positive as was first claimed in chapter 4. The functions g and g_t alone don't say much about the perturbations behaviour in time. However one can set up the equations for the reservoir, i.e. the IPR curve, and try to confirm the expression of function f from (4.19). It is clear the inflow performance relation (IPR) curve from the reservoir side, is essential in broadening the stability region of the TPR curve. The next chapter will summarize the work and present the conclusions.

CONCLUSIONS

The tubing performance relation (TPR) curve was introduced as a way to asses the performance of a gas well. Where the gas well transporting gas as well as liquid is just a small element of the whole production system. Under further inspection the TPR curve seems to be the collection of steady state solutions to the one dimensional two-phase flow problem. These steady state solutions are all possible natural production conditions. As many factors can effect the production a collection of stable production points would be desirable. Convention claims that the stable production conditions are located on the TPR curve to the right of the minimum. The argumentation for this claim is intuitive and thus mathematically weak. This report has set up a model to test this claim with perturbation analysis.

The TPR curve was approximated first with numerical integration and then with the pseudo-incompressibility assumption. The parameters f, C_0, u_b and μ where assumed constant. While these are flow regime or in the case of μ fluid dependent and would slightly change the shape of the TPR curve. Adding this dependence to the model would be an interesting next step to the research. Furthermore the relation between the superficial gas flow and the superficial liquid flow can be researched to present a more realistic representation. In reality the liquid could even move in the opposite direction to the gas. This might give a better representation of the liquid build up at the bottom of the well, described by liquid loading.

Another interesting idea is to model the problem with α as one of the unknown variables. This way the problem is less about the stable region of the TPR curve and more about the stability criteria of two-phase pipe flow. The advantage is that this α should better describe the turbulent flow regimes and give a more realistic representation of the flow. It would be interesting to see how a turbulent flow would effect the stability criteria.

After the TPR curve was approximated a small perturbation was added to a arbitrary point on the TPR curve. Two techniques for linearization were applied both resulting in the same final model for the perturbation. As the model depended on the steady state solutions the pseudo-incompressibility assumption greatly simplified the equations describing the behaviour of the perturbation. For low Mach numbers, i.e. low flow rates, the assumption is valid. It showed that around the minimum of the TPR curve this assumption would be valid. It is still a good idea to test the assumption that $c_g \gg u_{max}$, where $c_g = zRT$ and u_{max} is the maximum possible flow rate, for actual gas well data.

After projecting the perturbation on a basis the behaviour of the basis vectors was studied. The flow to the right of the minimum of the TPR curve was indeed stable, while the flow to the left was unstable. This conclusion is assumed to also hold in the case that pseudo-incompressibility is not applied. Take note however that the expression for the tangent of the TPR curve then also changes and the relation between ω and the tangent might not be as straightforward. However the difference between both method should be of order ε and no problems are expected.

Lastly while the traditional claim of the stable region of the TPR has been verified, the claim of a possible stable region slightly left of the TPR curve is not. The combined curve $f - g$ from chapter 4 can not be linked to the linearization (5.39) and (5.40) from chapter 5. After all, the conservation equations used to model them are specific to the well part of the well-reservoir system. As such the tangent of the combined curved will not present itself in an expression for stability variable ω. However the linearization can be expanded on, by using the transfer function. If the transfer function for the reservoir side of the system is known then it may be combined with the transfer function of the well. Then the claim about a larger stability region can be tested. This would indeed prove interesting even though it might not be practical. The stable region left of the minimum would be dependent on the IPR curve and vary for every system. Furthermore a stable region does not guarantee a natural production point is present in this region.

A

DEFINITIONS: MATH

Definition A.1 (Operator)**.** An operator F is a mapping from one vector space to another, i.e. $F : V \to W$ with V and W vector spaces.

Definition A.2 (Fréchet derivative)**.** Given V, W Banach spaces and $U \subset V$ the operator $f : U \to W$ has a Fréchet derivative Df_x in x, if $\exists$ a linear operator $A_x : V \to W$ such that

$$\lim_{h \to 0} \frac{\|f(x+h) - f(x) - A_x h\|_W}{\|h\|_V} = 0. \tag{A.1}$$

Then $Df(x) := A_x$

A weaker version of the Fréchet derivative is the Gâteaux derivative.

Definition A.3 (Gâteaux derivative)**.** Given the Banach spaces V, W, the Gâteaux derivative of an operator $F : U \subset V \to W$ is given by

$$\mathrm{d}_h f(x) = \lim_{t \to 0} \frac{f(x+th) - f(x)}{t} \tag{A.2}$$

B

DEFINITIONS: THEORY

Definition B.1 (Inviscid flow)**.** Is the flow of an ideal fluid with no viscosity. A fluid flow may be assumed inviscid if the viscous forces are small with respect to the inertial forces. A way to measure the viscous forces versus the inertial forces is the Reynolds number, Re. If the Reynolds number is much larger than one, $Re \gg 1$, the flow may be assumed inviscid.

Definition B.2 (Laminar flow)**.** Non-turbulent flow. A contour plot of this type of flow would have no flow lines mixing and/ or crossing.

Definition B.3 (Newtonian fluid)**.** A fluid for which the shear stress τ can be expressed as

$$\tau = \mu \frac{\partial u}{\partial r} \tag{B.1}$$

With μ the fluid viscosity, u the flow rate and r the radial coordinate in a cylindrical coordinate system. Where the direction of the flow rate u is parallel to the shear stress τ. While the direction y is perpendicular to the shear stress τ.

C

THE MECHANICAL ENERGY EQUATION

The mechanical energy is the sum of the kinetic and the potential energy of an object. In this case the object is the fluid. The equation for the kinetic energy is known as,

$$E_k = \rho V \frac{v^2}{2}, \tag{C.1}$$

where ρ, V and v are the density, volume and velocity respectively. The potential energy is a bit more complicated and can be a combination of the gravitational energy, the pressure and work. The mechanical energy between to points is given by

$$\frac{p_1}{\rho} + gz_1 + \frac{v_1^2}{2} = \frac{p_2}{\rho} + gz_2 + \frac{v_2^2}{2} + W + E_l. \tag{C.2}$$

Where W is the work done on the system. And E_l is the irreversible energy losses, which given flow in a pipe is linked to the frictional force. Assuming $W = 0$ no work is done on/ by the system one may rewrite the mechanical energy equation.

$$\frac{\Delta p}{\rho} + g\Delta z + \frac{\Delta(v^2)}{2} + \frac{f\rho v^2 dz}{2D} = 0. \tag{C.3}$$

Deviding the above equation and taking the limit $\Delta z \to 0$ results in the steady state momentum conservation equation,

$$\frac{\partial_z p}{\rho} + g + v\partial_z v + \frac{f\rho v^2}{2D} = 0. \tag{C.4}$$

BIBLIOGRAPHY

[1] R. Oliemans, *Applied Multiphase Flows: AP3181D* (TU Delft, 2007).

[2] J. Lea, H. Nickens, and M. Wells, *Gas Well Deliquification: Solutions to Gas Well Liquid Loading Problems*, Gulf drilling guides (Elsevier Science, 2003).

[3] J. Jansen and P. Currie, *Modelling and Optimisation of Oil and Gas Production Systems* (TU Delft, 2004).

[4] W. Lee and R. Wattenbarger, *Gas Reservoir Engineering*, SPE textbook series (Soc. of Petroleum Engineers, 1996).

[5] B. Guo, W. Lyons, and A. Ghalambor, *Petroleum Production Engineering* (Eslsevier Science & Technology Books, 2007).

[6] C. Colebrook, *Turbulent flow in pipes with particular reference to the transition region between the smooth and rough pipe laws,,* Journal of the ICE **11**, 133 (1939).

[7] S. Churchill, *Friction-factor equation spans all fluid-flow regimes,* Chemical Engineering **7**, 91 (1977).

[8] T. Bergman, A. Lavine, and F. Incropera, *Fundamentals of Heat and Mass Transfer, 7th Edition* (John Wiley & Sons, Incorporated, 2011).

[9] D. Pugliesi, *Generalized diagram of compressipility factor (z=pv/rt)*. Wikipedia (2008).

[10] N. Zuber and J. Findlay, *Average volumetric concentration in two-phase flow systems,* Journal of Heat Transfer **87**, 453 (1965).

[11] M. Ishii, *One-dimensional drift-flux model and constitutive equations for relative motion between phases in various two-phase flow regimes,* Argonne National Lab Report **47** (1977).

[12] T. Hibiki and M. Ishii, *One-dimensional drift–flux model for two-phase flow in a large diameter pipe,* International Journal of Heat and Mass Transfer **46**, 1773 (2003).

[13] C. Brennen, *Fundamentals of Multiphase Flow* (Cambridge University Press, 2005).

[14] F. Verhulst, *Nonlinear Differential Equations and Dynamical Systems*, Universitext (Springer Berlin Heidelberg, 2006).

NOMENCLATURE

$\mathbf{F}$	net body forces vector, N
$\mathbf{u}$	flow rate vector, $\mathrm{m\,s^{-1}}$
μ	Fluid viscosity, Pa s
ρ	density, $\mathrm{kg\,m^{-3}}$
τ_w	shear stress at the well wall, $\mathrm{kg\,m^{-1}\,s^{-2}}$
θ	angle of the well, [-]
ε	absolute roughness, [-]
A	cross section of the well, $\mathrm{m^2}$
C_0	distribution correlation, [-]
E	total energy, J
Fr	Froude number, [-]
g	gravitational acceleration, $\mathrm{m\,s^{-2}}$
M	Mach number, [-]
p	pressure, $\mathrm{kg\,m^{-1}\,s^{-2}}$
Q	mass flow rate, $\mathrm{kg\,s^{-1}}$
R	specific gas constant, $\mathrm{J\,kg^{-1}\,K^{-1}}$
S	perimeter of the well, m
T	temperature, K
u	flow rate, $\mathrm{m\,s^{-1}}$
u_b	weighted mean drift flow rate, $\mathrm{m\,s^{-1}}$
z	compressibility factor, [-]